Few notes on the dynamics of Flaviviruses in Brazil

Grandes Endemias

Paolo Zanotto, D. Phil.

Life Cycle of DENV

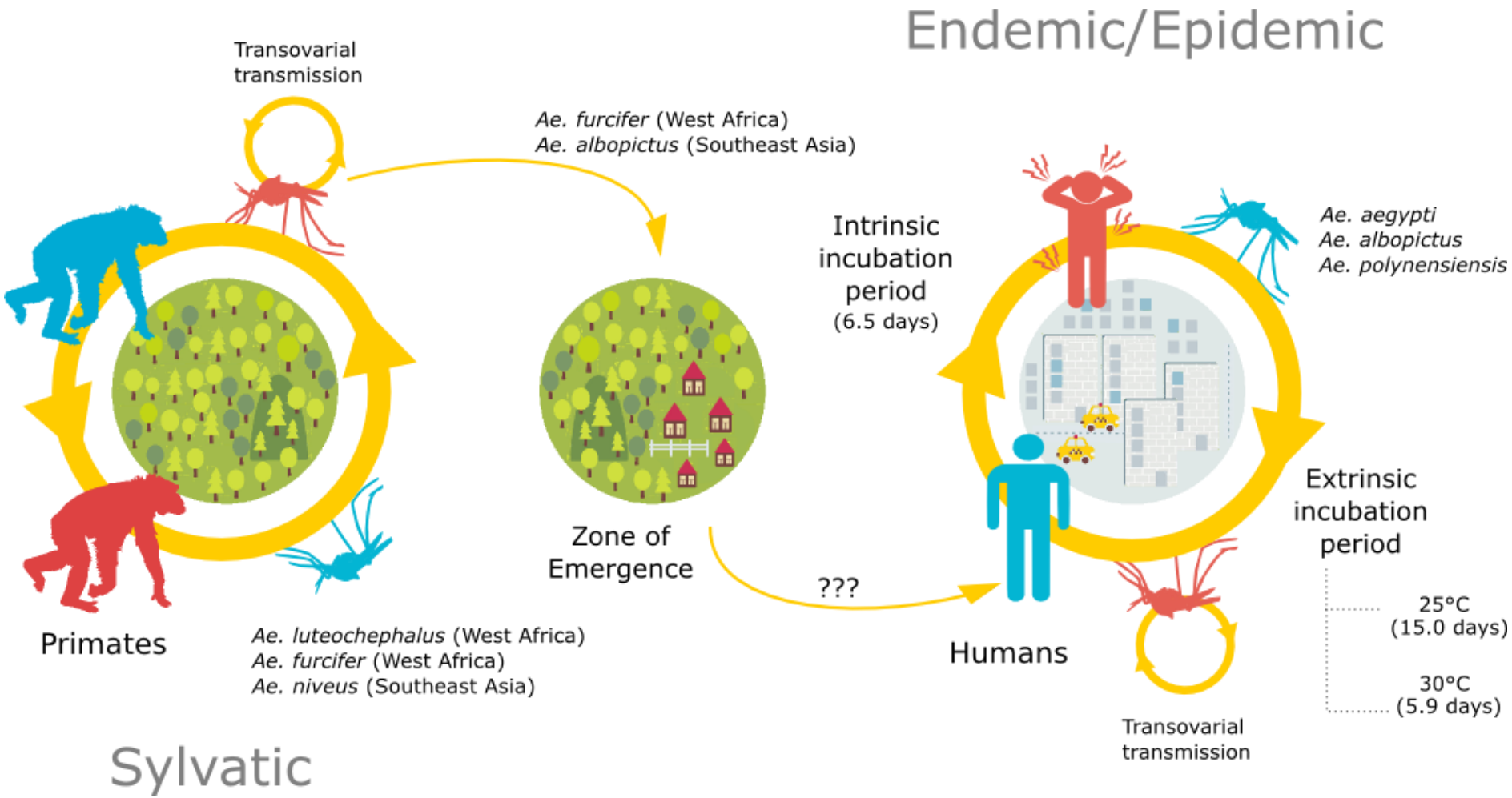

Flavivirus genome

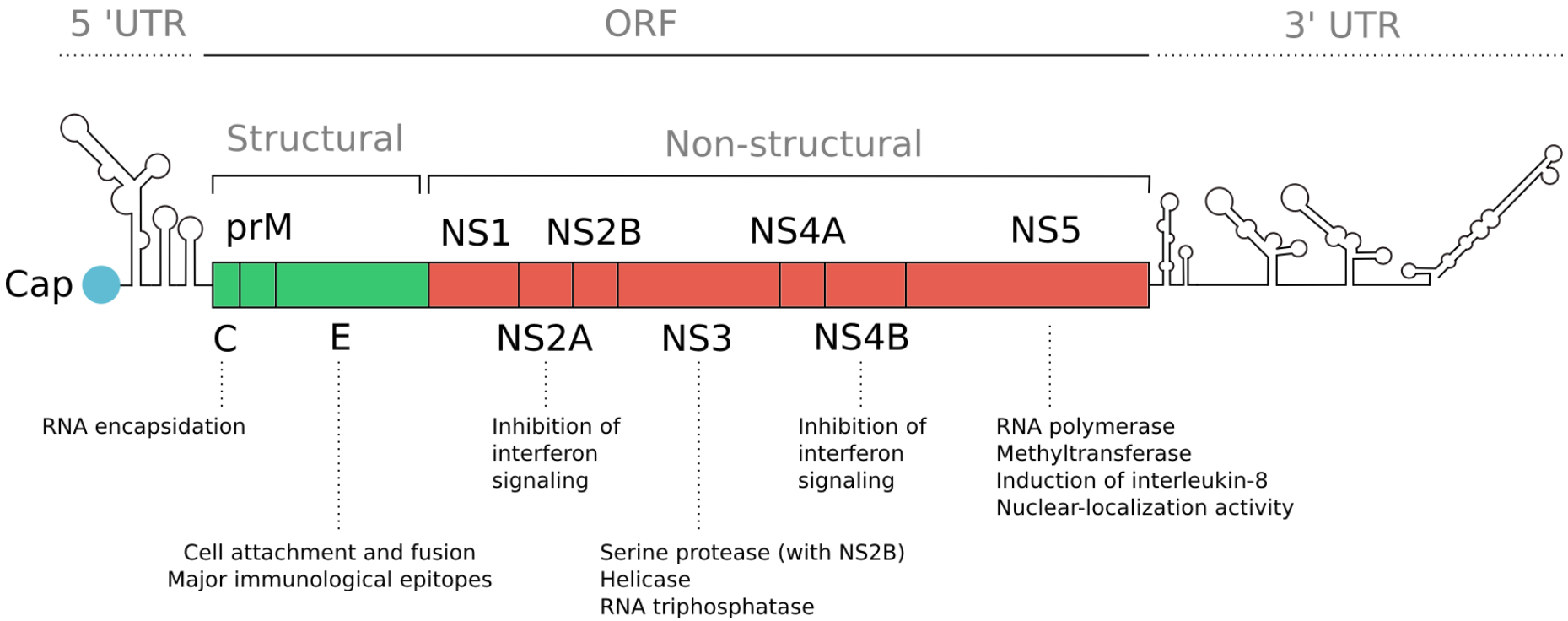

DENV worldwide burden

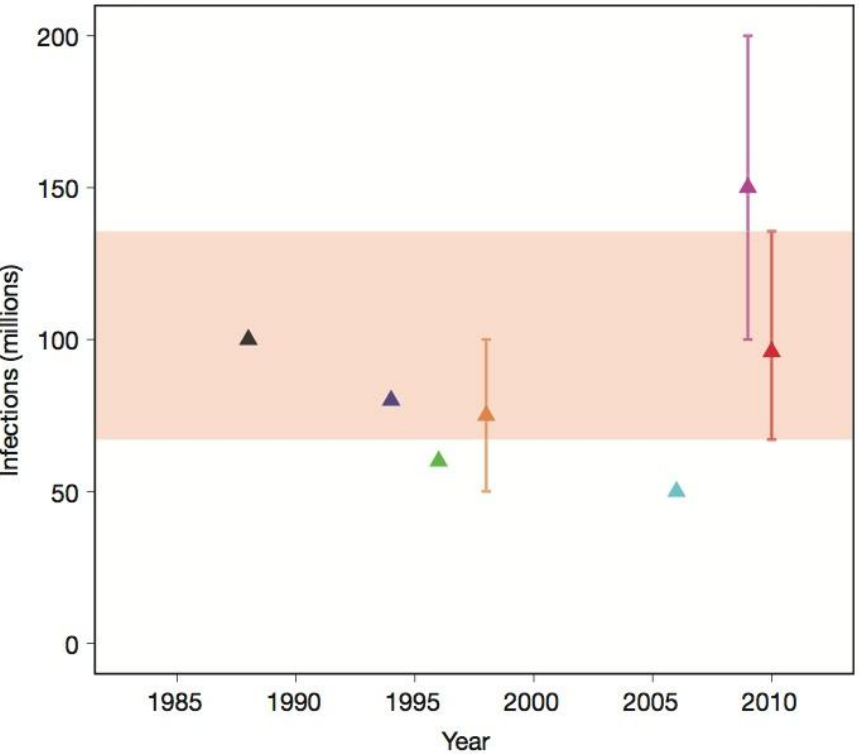

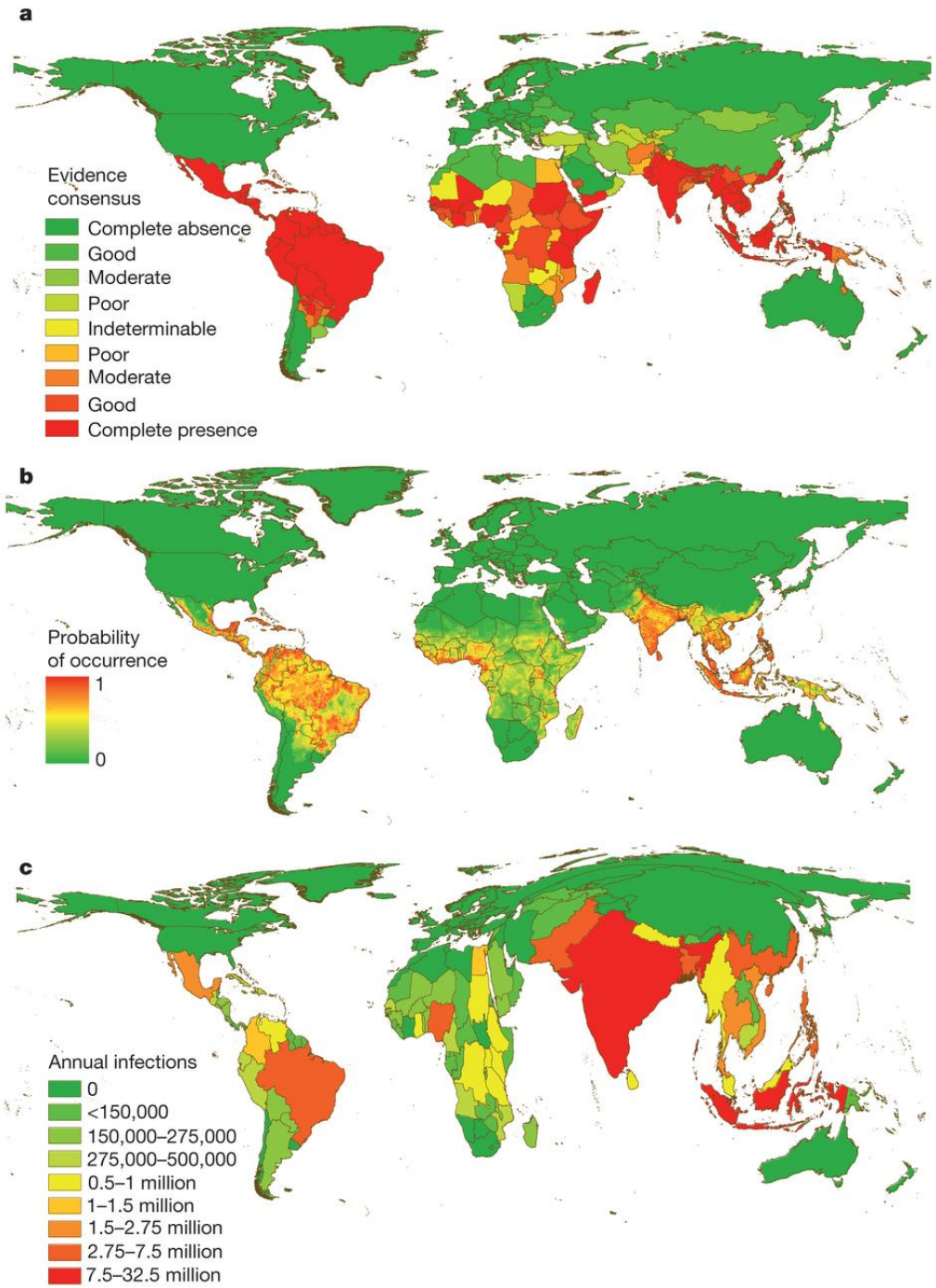

DENV in SP

Casos notificados

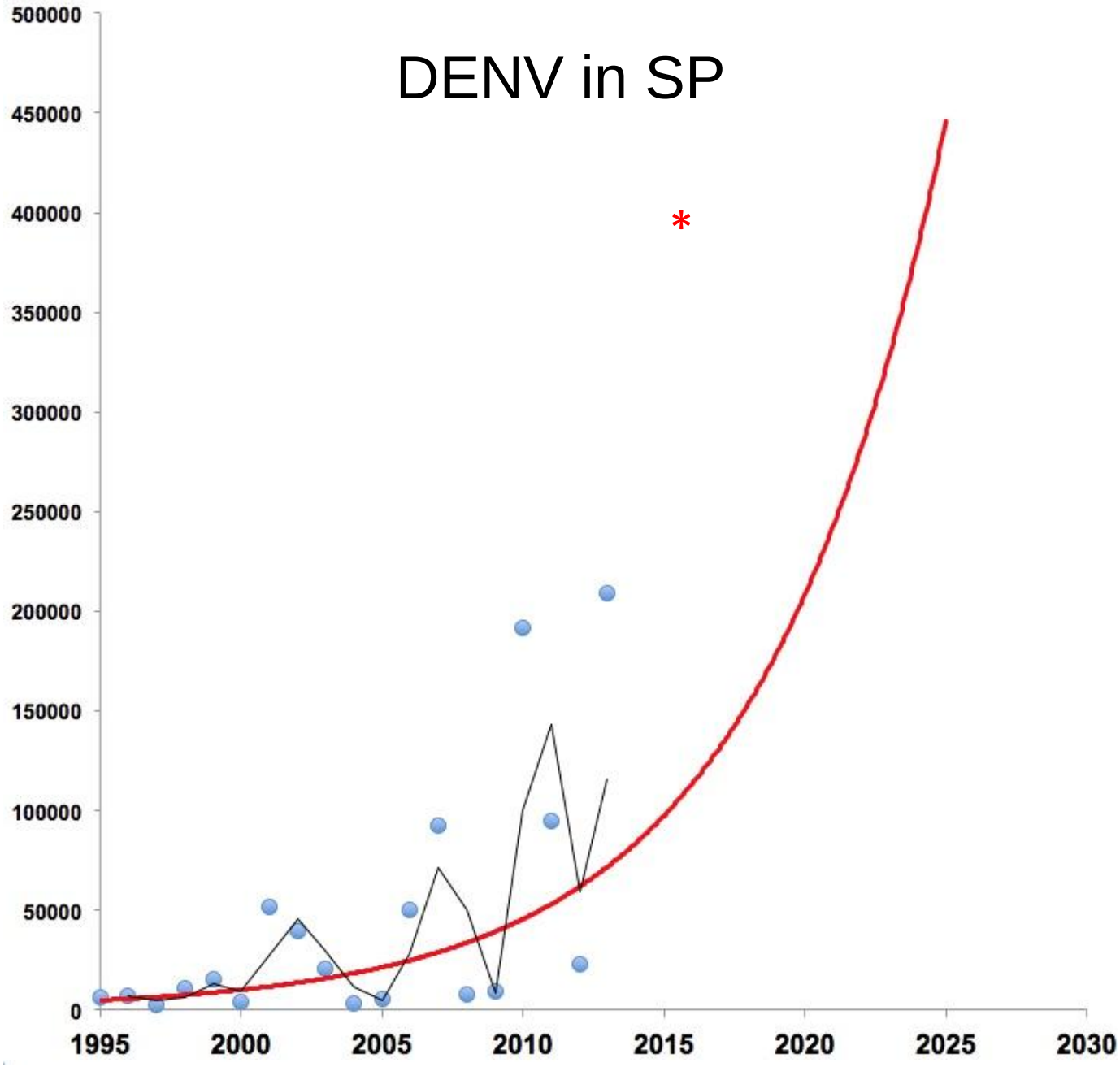

OPEN ACCESS Freely available online

PLoS NEGLECTED TROPICAL DISEASES

Spatio-Temporal Tracking and Phylodynamics of an Urban Dengue 3 Outbreak in São Paulo, Brazil

Adriano Mondini[1], Roberta Vieira de Moraes Bronzoni[1], Silvia Helena Pereira Nunes[1], Francisco Chiaravalloti Neto[1,2], Eduardo Massad[3], Wladimir J. Alonso[4], Eduardo S. M. Lázzaro[5], Amena Alcântara Ferraz[5], Paolo Marinho de Andrade Zanotto[6], Maurício Lacerda Nogueira[1]*

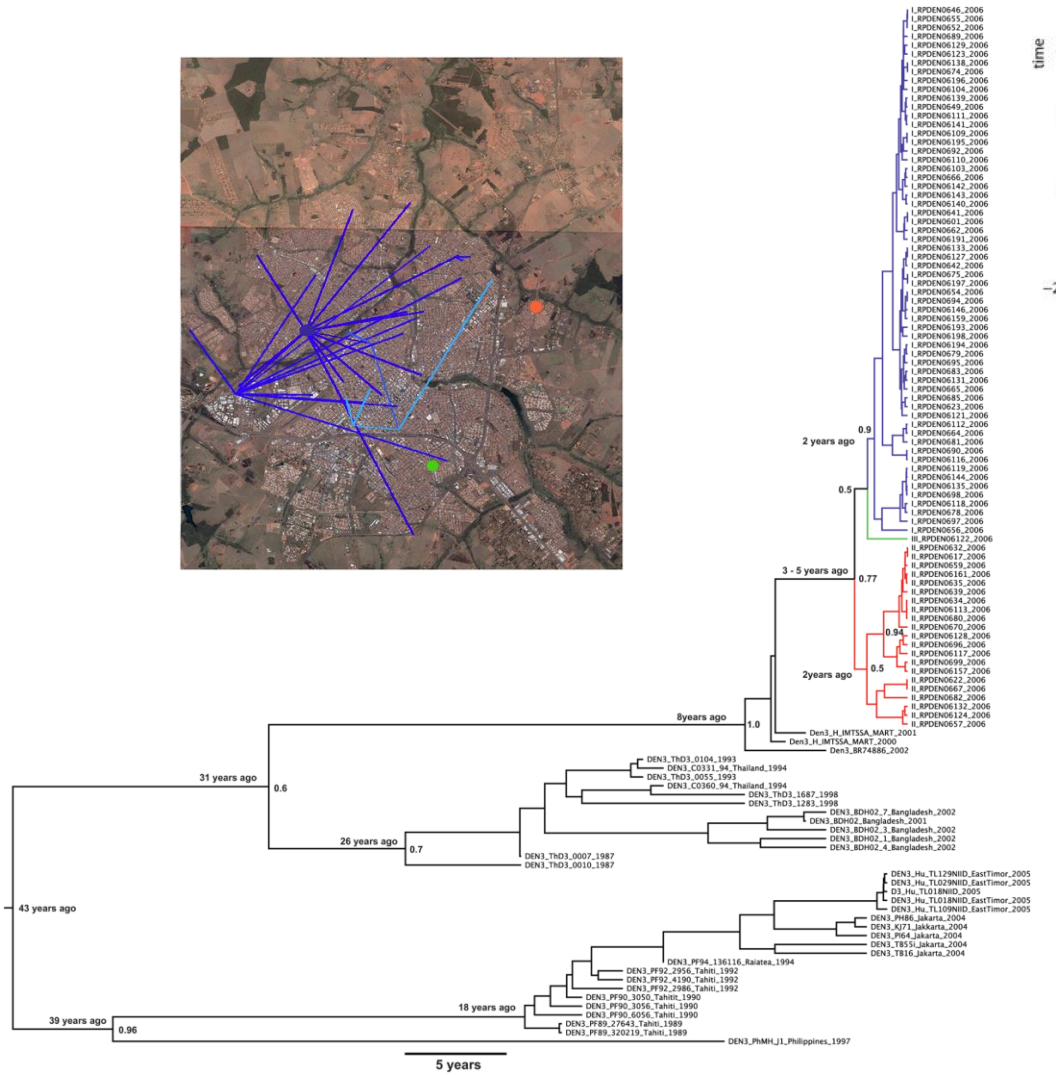

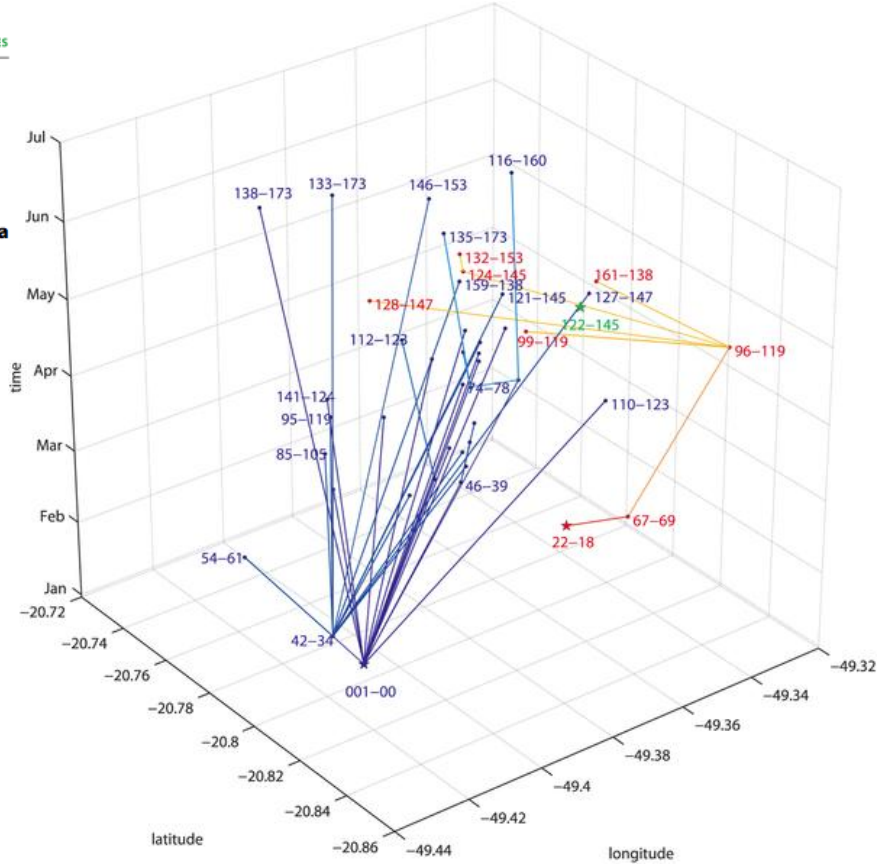

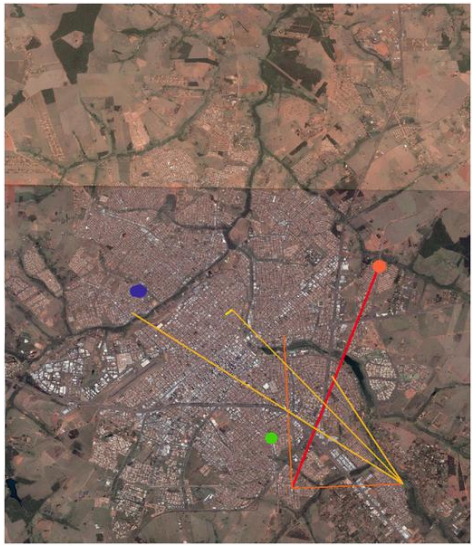

OPEN ACCESS Freely available online

PLOS | NEGLECTED TROPICAL DISEASES

Viewpoints

Detection of Four Dengue Serotypes Suggests Rise in Hyperendemicity in Urban Centers of Brazil

Christian Julián Villabona-Arenas[1], Jessica Luana de Oliveira[1], Carla de Sousa Capra[2], Karime Balarini[3], Mauricio Loureiro[4], Celso Ricardo Theoto P. Fonseca[3], Saulo Duarte Passos[4], Paolo Marinho de Andrade Zanotto[1]*

1 Laboratório de Evolução Molecular e Bioinformática, Departamento de Microbiologia, Instituto de Ciências Biomédicas, Universidade de São Paulo, São Paulo, São Paulo, Brazil, **2** Laboratório de Saúde Pública, Secretaria da Saúde, Prefeitura Municipal de Guarujá, Guarujá, São Paulo, Brazil, **3** Itapema Laboratório de Análises Clínicas, Guarujá, São Paulo, Brazil, **4** Laboratório de Infectologia Pedriátrica, Faculdade de Medicina de Jundiaí, Jundiaí, São Paulo, Brazil

DENV-3 samples were from genotype V

- Genotype III has been the most prevalent in Brazil. However, genotypes I and V were associated with dengue outbreaks in Brazil.

- Cryptic circulation of DENV-3 in the region?

- A new introduction from Asia?

- Q: "What is the *A. aegypti* lineage in Santos?"
  R: "Singapore"!

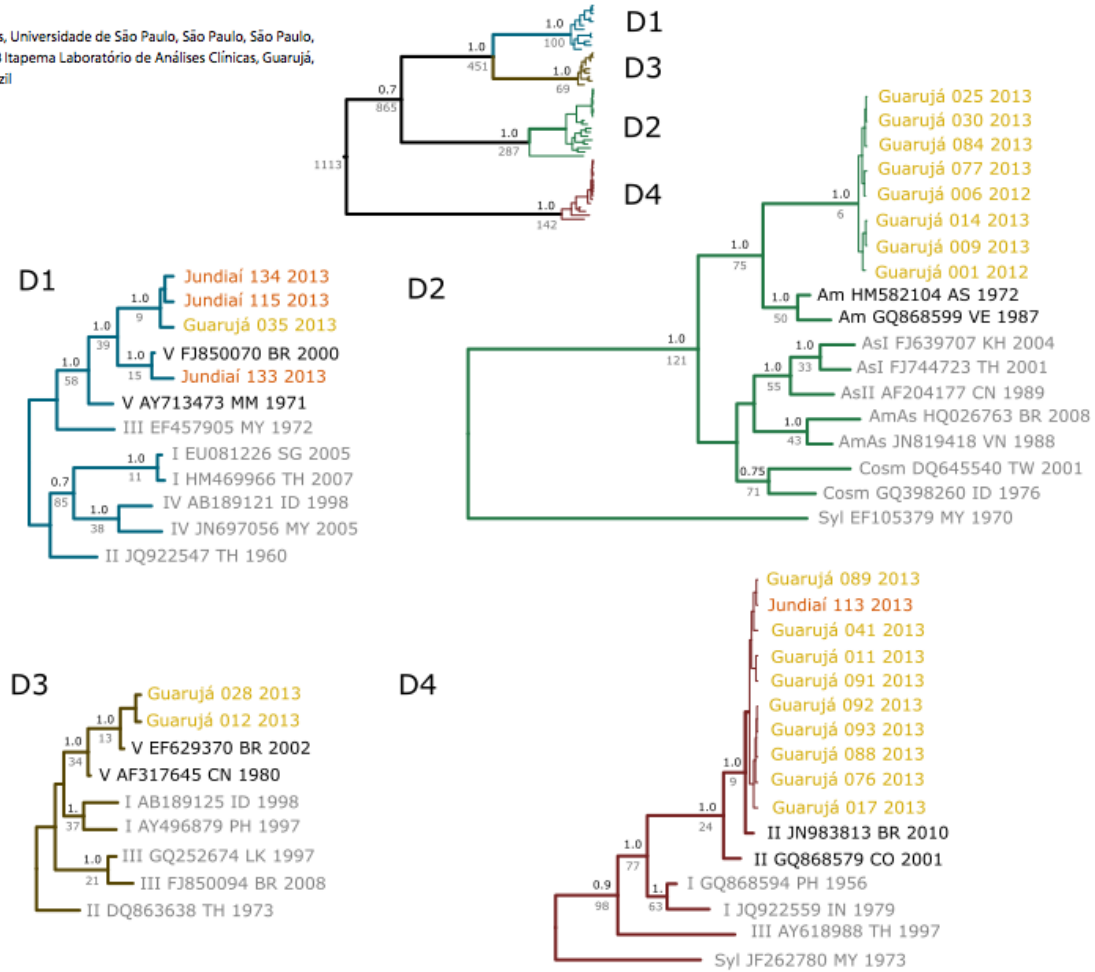

Figure 1. Maximum credibility tree (and its four serotype subtrees) showing the evolutionary relationships among the capsid/ premembrane junction sequences of 55 strains. Posterior probability support values are shown over the nodes and TMRCAs values below the nodes. Reference sequences abbreviated by serotype (D1–4), genotype (*Am*: American, *AmAs*: American/Asian, *As*: Asian, *Cosm*: Cosmopolitan, *Syl*: Sylvatic, *I*, *II*, *III*, *IV*, or *V*), GenBank accession, ISO code for country, and isolation year.
doi:10.1371/journal.pntd.0002620.g001

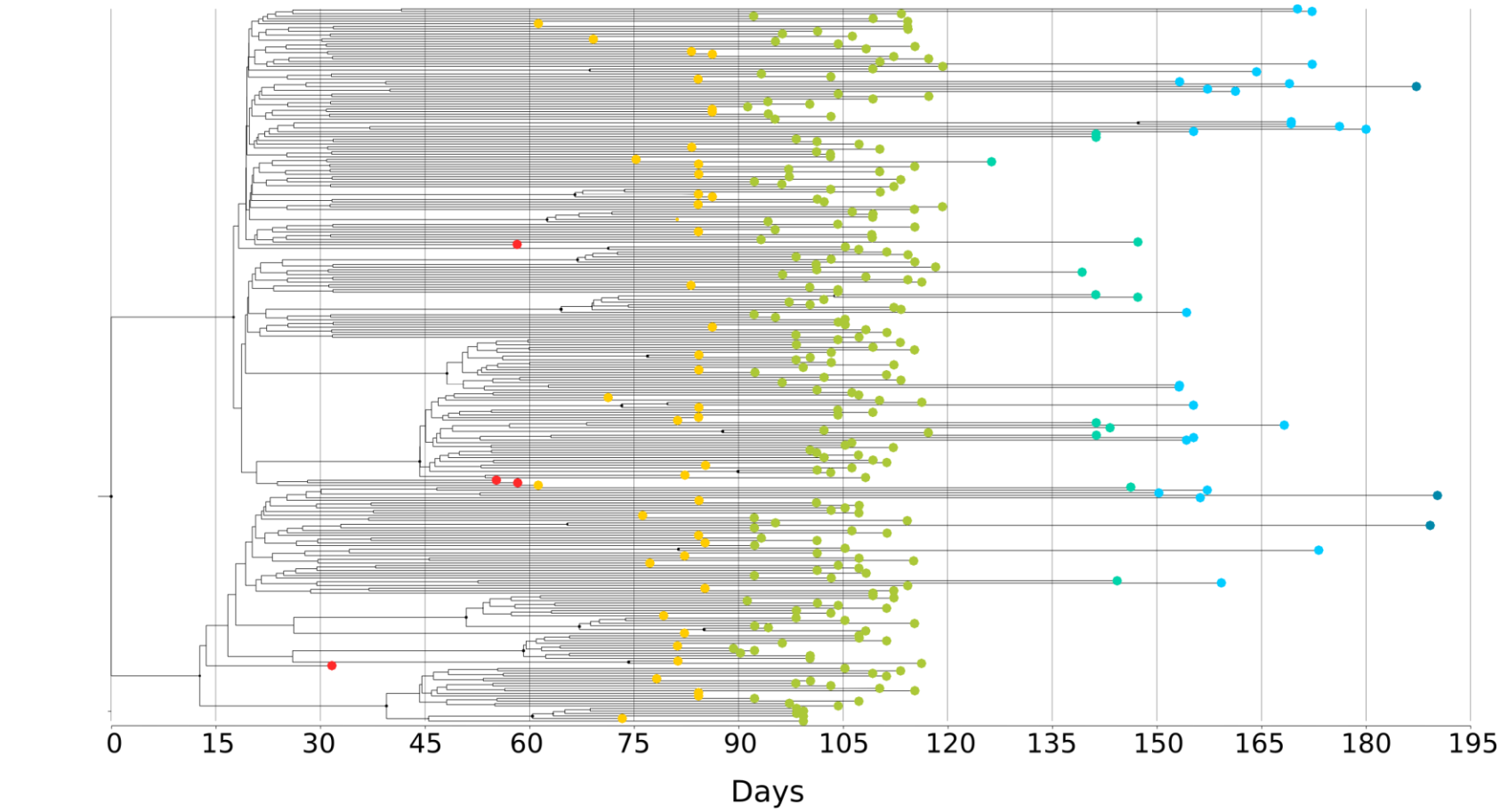
0
15
30
45
60
75
90
105
120
135
150
165
180
195
Days

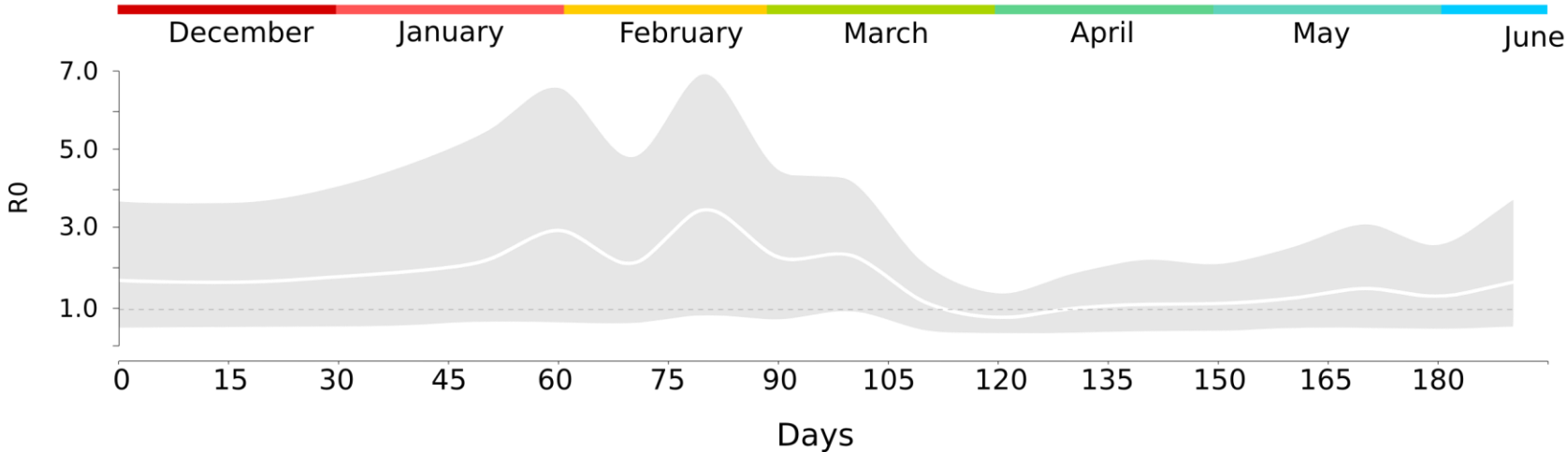
December
January
February
March
April
May
June
7.0
5.0
3.0
1.0
R0
0
15
30
45
60
75
90
105
120
135
150
165
180
Days

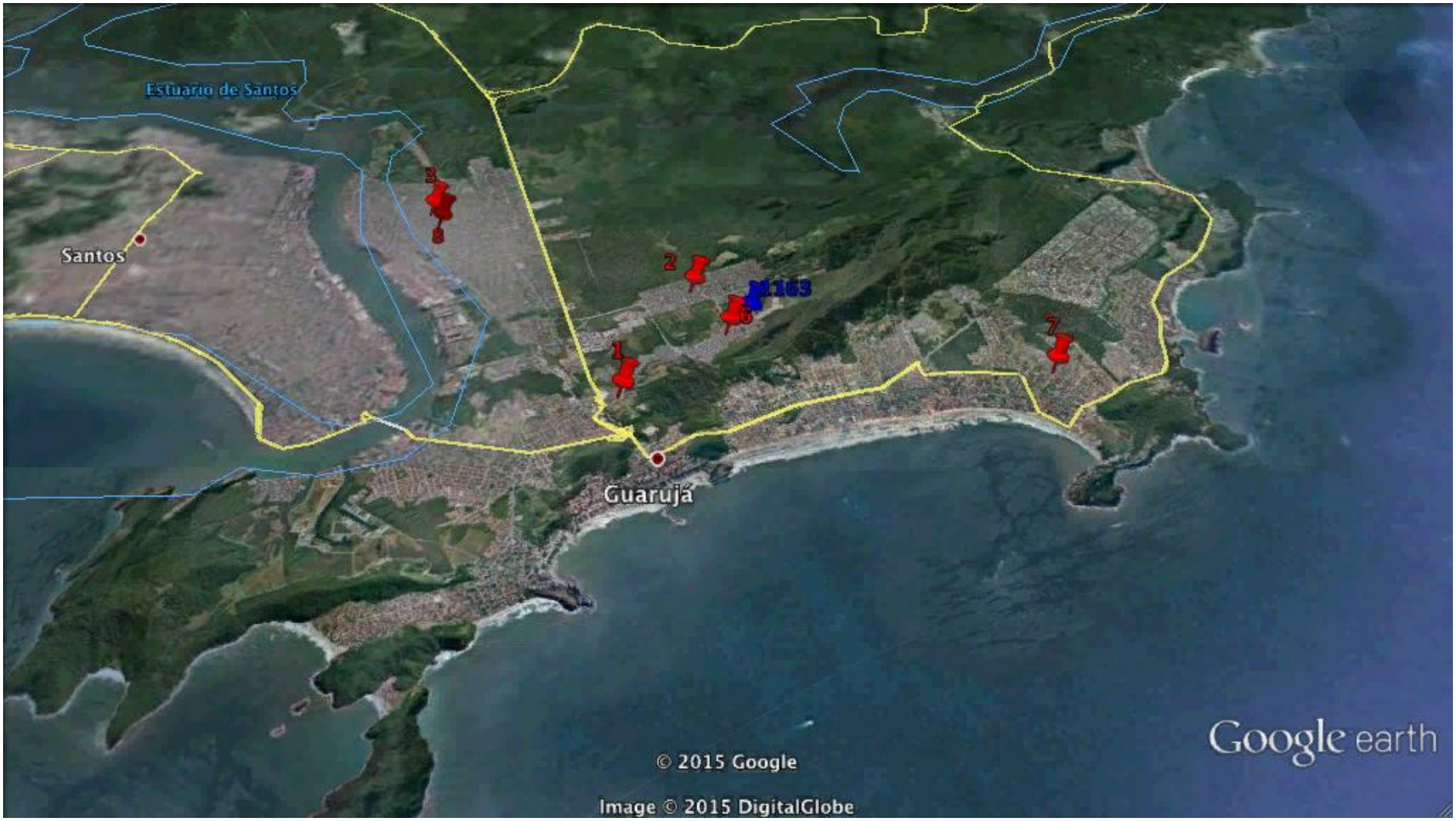

Days

December January February March April May June

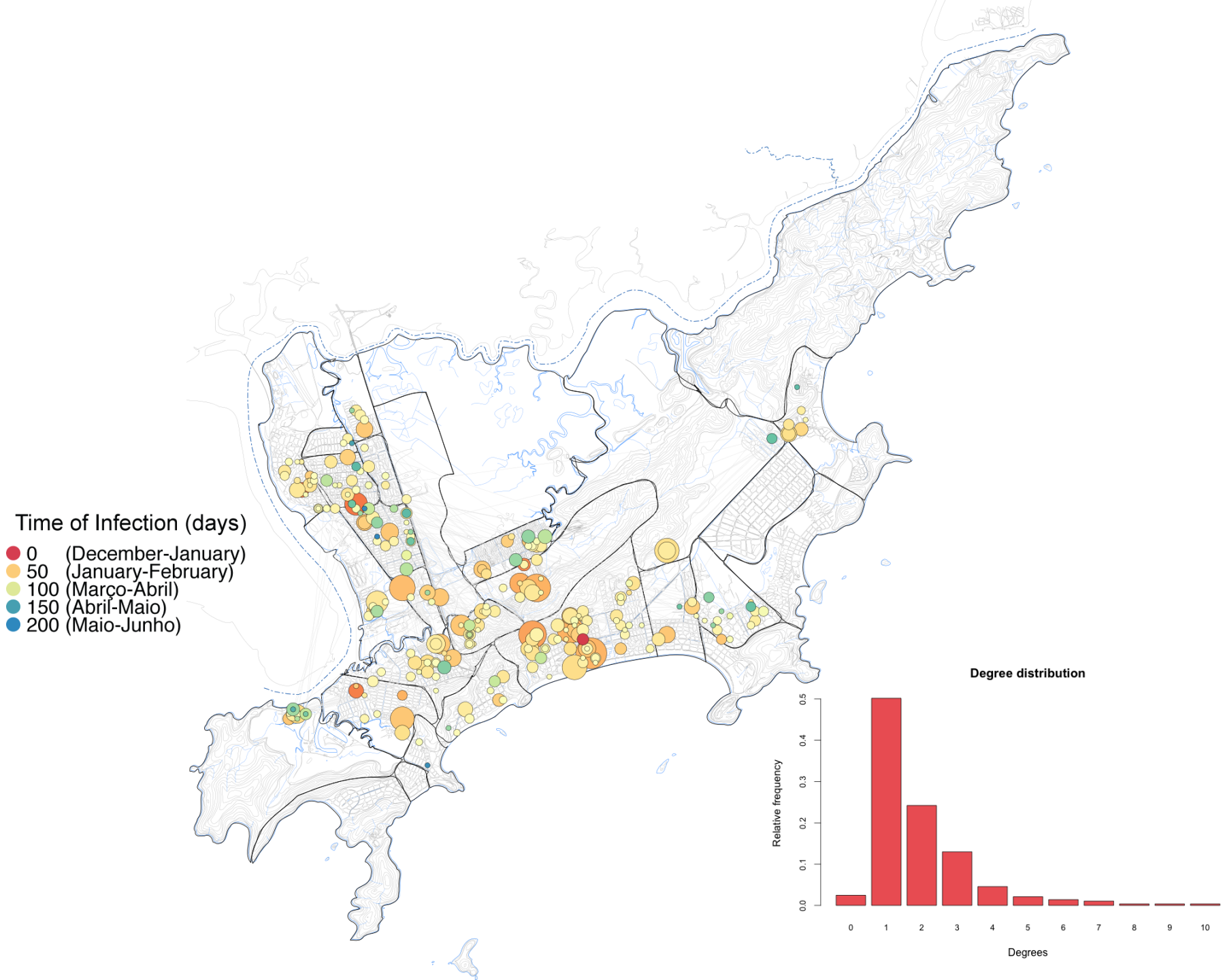
Time of Infection (days)
0 (December-January)
50 (January-February)
100 (Março-Abril)
150 (Abril-Maio)
200 (Maio-Junho)
Degree distribution
Relative frequency
0.0
0.1
0.2
0.3
0.4
0.5
0
1
2
3
4
5
6
7
8
9
10
Degrees

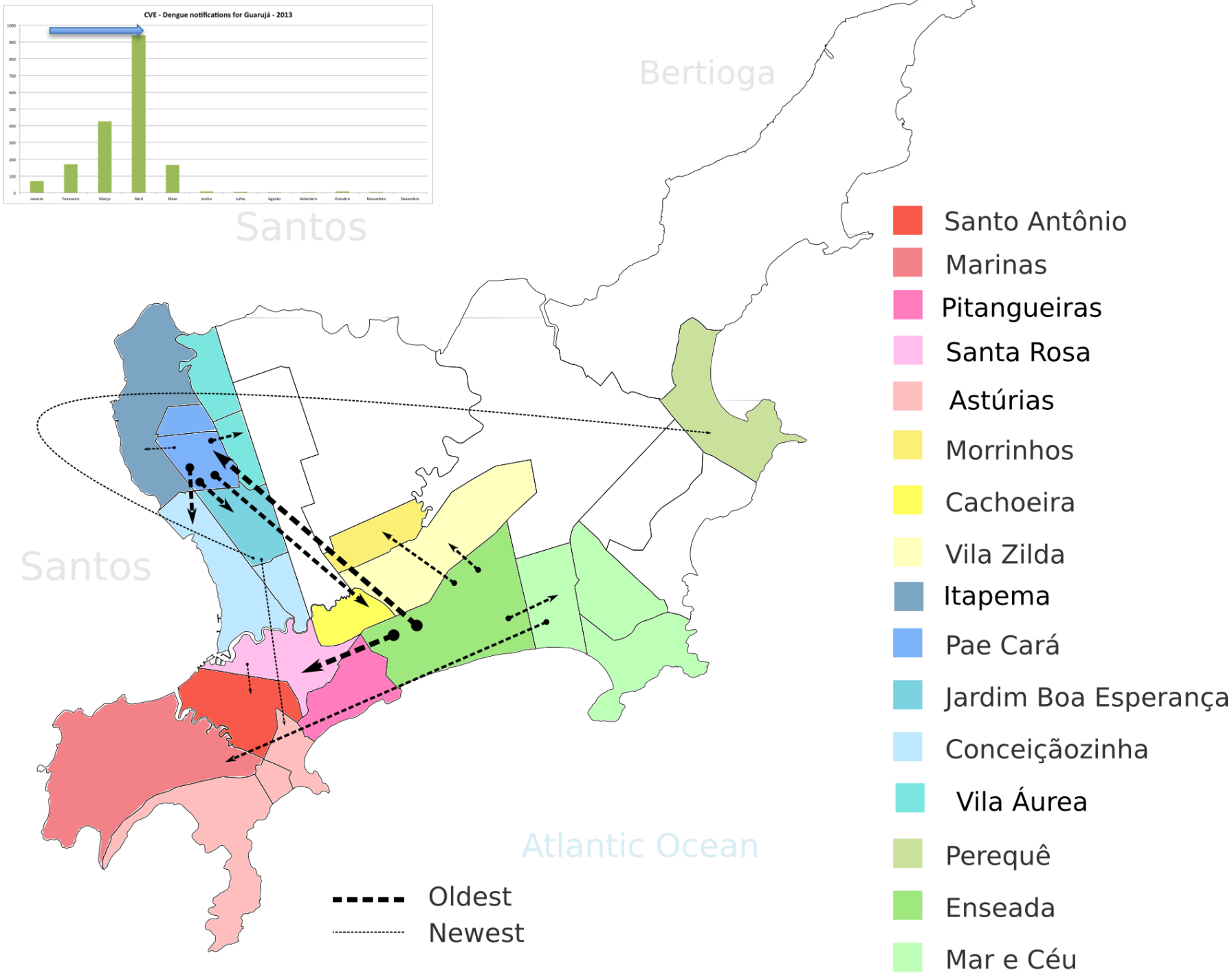
CVE - Dengue notifications for Guarujá - 2013
1000
900
800
700
600
500
400
300
200
100
0
Janeiro
Fevereiro
Março
Abril
Maio
Junho
Julho
Agosto
Setembro
Outubro
Novembro
Dezembro
Bertioga
Santos
Santos
Atlantic Ocean
Oldest
Newest
Santo Antônio
Marinas
Pitangueiras
Santa Rosa
Astúrias
Morrinhos
Cachoeira
Vila Zilda
Itapema
Pae Cará
Jardim Boa Esperança
Conceiçãozinha
Vila Áurea
Perequê
Enseada
Mar e Céu

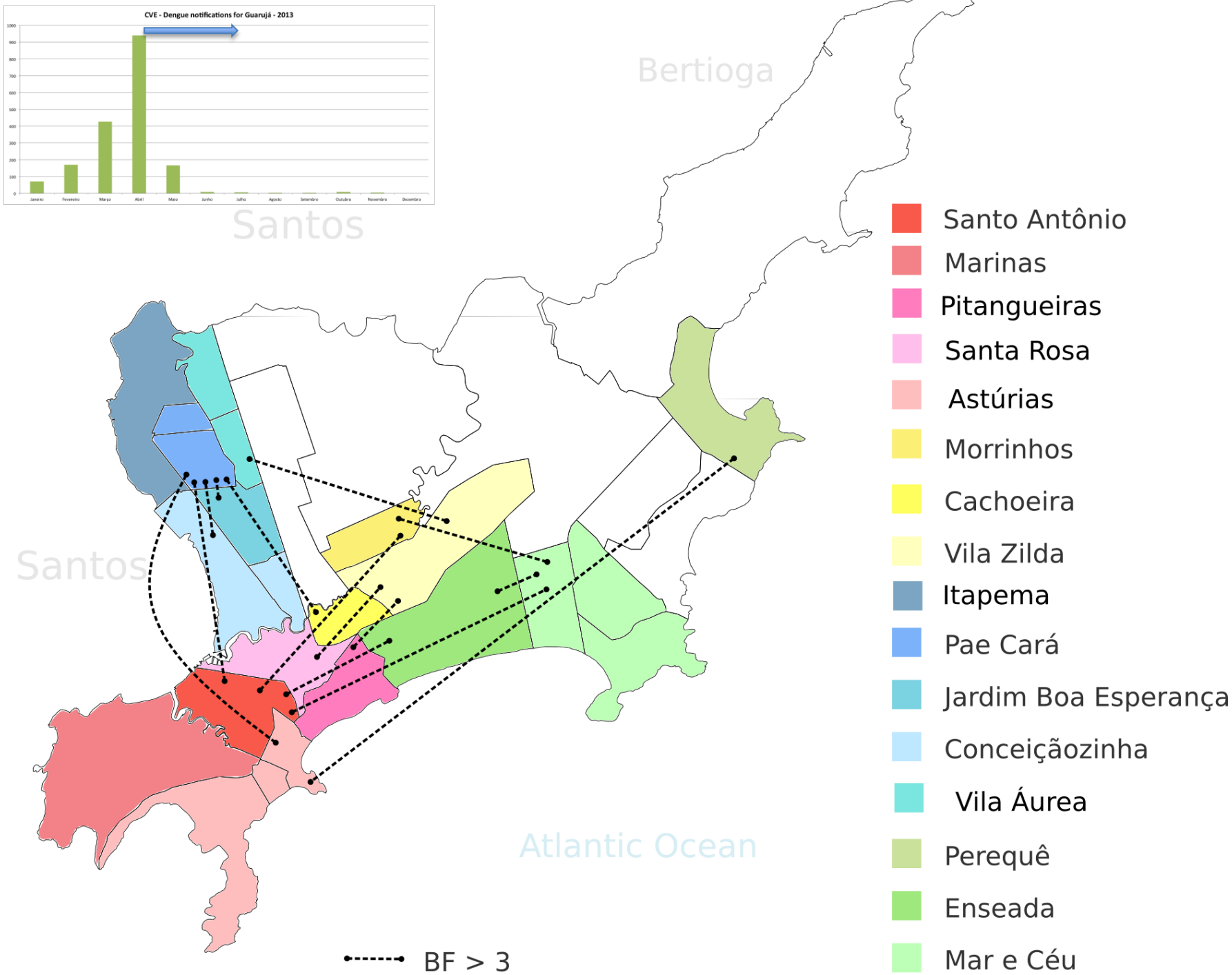
CVE - Dengue notifications for Guarujá - 2013
1000
900
800
700
600
500
400
300
200
100
0
Janeiro
Fevereiro
Março
Abril
Maio
Junho
Julho
Agosto
Setembro
Outubro
Novembro
Dezembro
Bertioga
Santos
Santos
Atlantic Ocean
Santo Antônio
Marinas
Pitangueiras
Santa Rosa
Astúrias
Morrinhos
Cachoeira
Vila Zilda
Itapema
Pae Cará
Jardim Boa Esperança
Conceiçãozinha
Vila Áurea
Perequê
Enseada
Mar e Céu
BF > 3

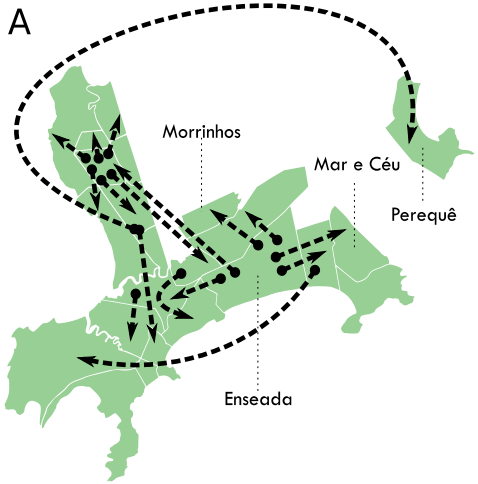

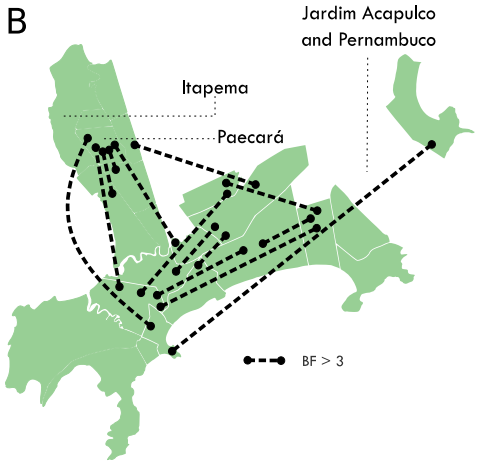

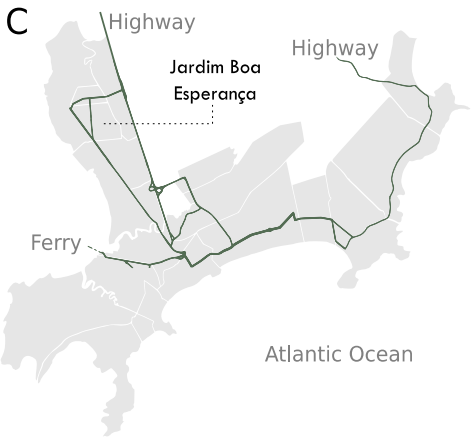

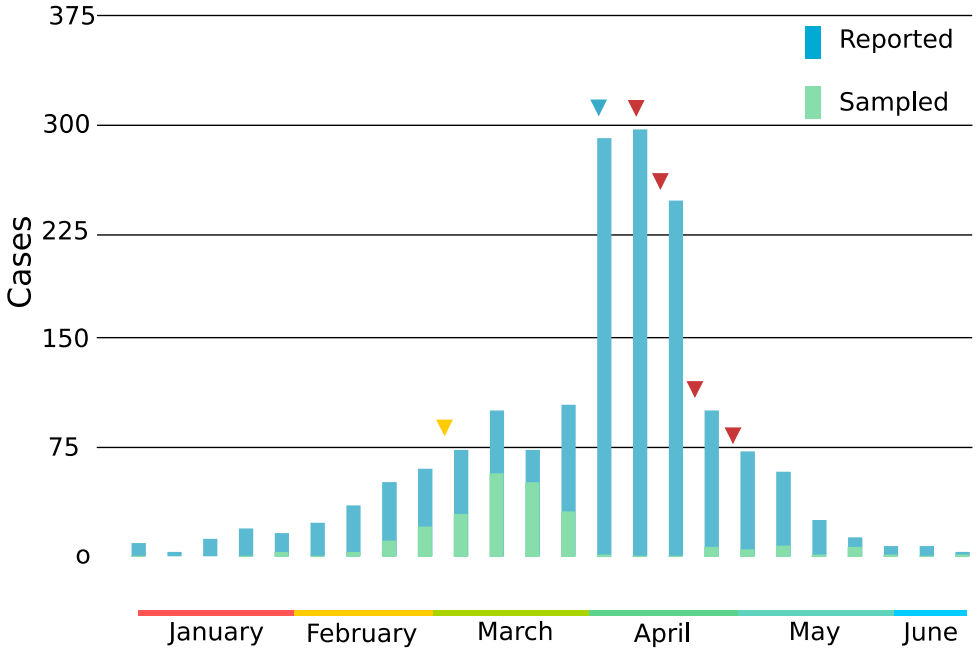

Blue: epidemiological situation.
Yellow: source reduction initiatives in shantytowns started.
Red: insecticide

DENV4 - Transmission Network

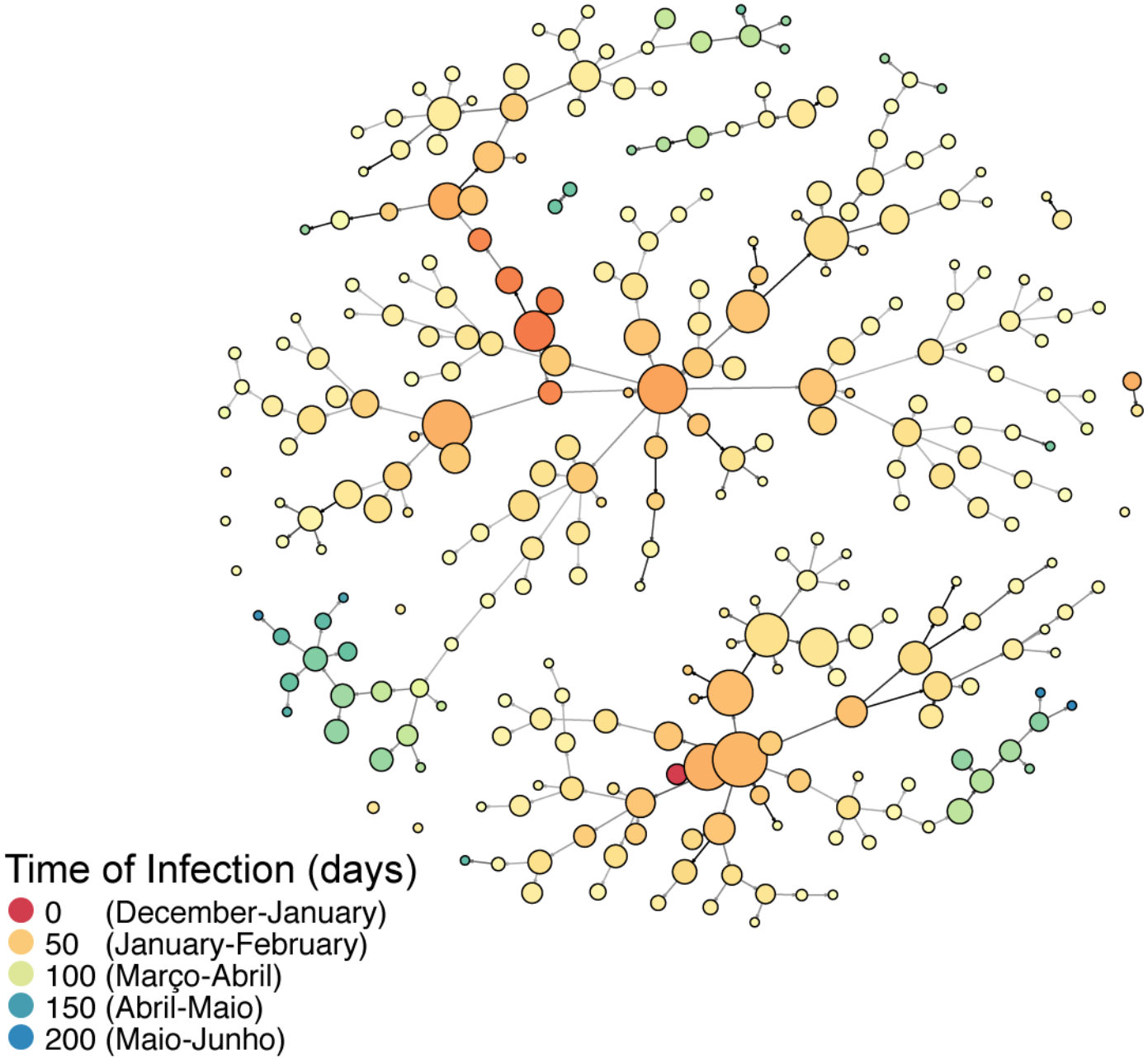

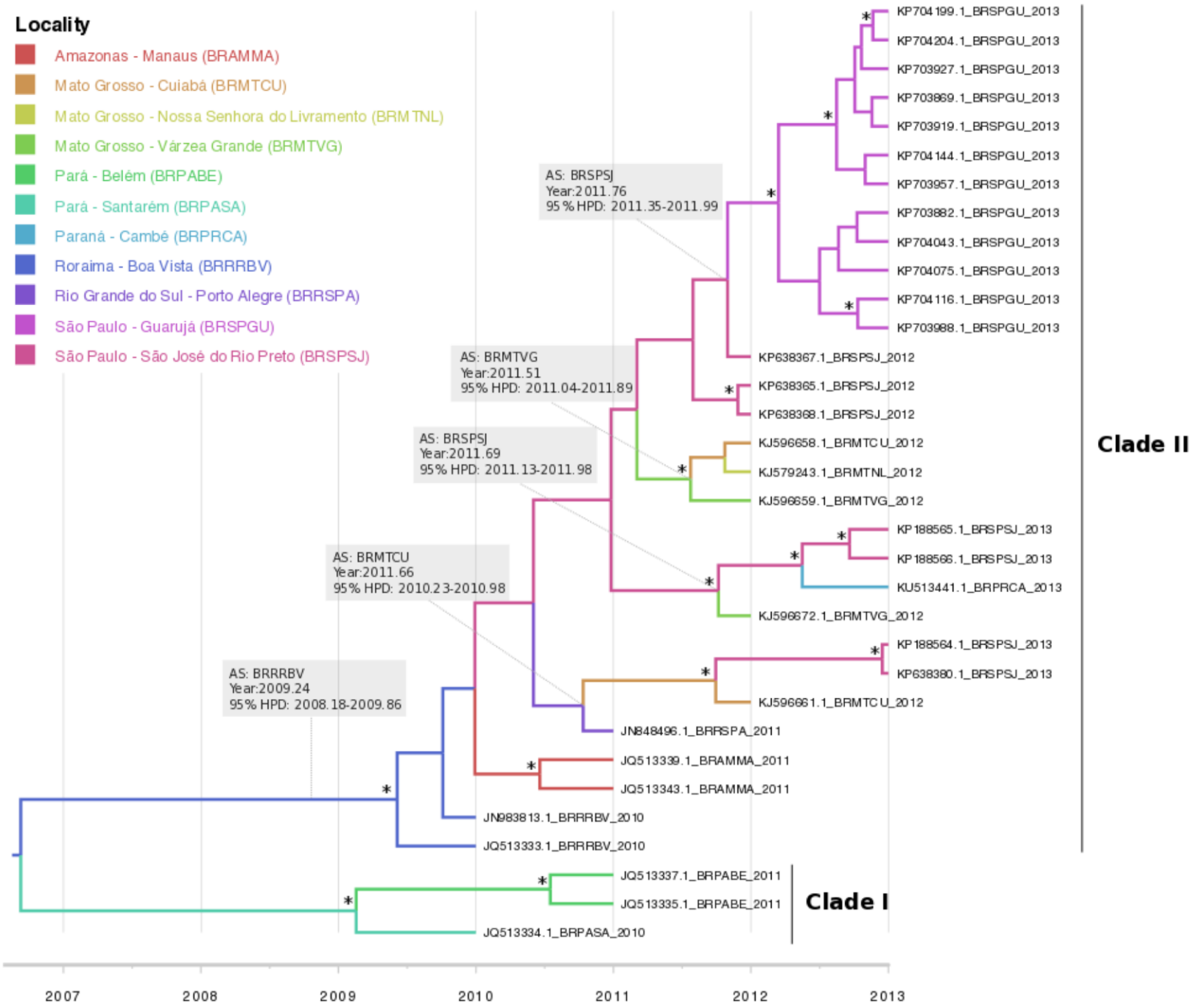
Locality
Amazonas - Manaus (BRAMMA)
Mato Grosso - Cuiabá (BRMTCU)
Mato Grosso - Nossa Senhora do Livramento (BRMTNL)
Mato Grosso - Várzea Grande (BRMTVG)
Pará - Belém (BRPABE)
Pará - Santarém (BRPASA)
Paraná - Cambé (BRPRCA)
Roraima - Boa Vista (BRRRBV)
Rio Grande do Sul - Porto Alegre (BRRSPA)
São Paulo - Guarujá (BRSPGU)
São Paulo - São José do Rio Preto (BRSPSJ)
AS: BRSPSJ
Year:2011.76
95% HPD: 2011.35-2011.99
AS: BRMTVG
Year:2011.51
95% HPD: 2011.04-2011.89
AS: BRSPSJ
Year:2011.69
95% HPD: 2011.13-2011.98
AS: BRMTCU
Year:2011.66
95% HPD: 2010.23-2010.98
AS: BRRRBV
Year:2009.24
95% HPD: 2008.18-2009.86
KP704199.1_BRSPGU_2013
KP704204.1_BRSPGU_2013
KP703927.1_BRSPGU_2013
KP703869.1_BRSPGU_2013
KP703919.1_BRSPGU_2013
KP704144.1_BRSPGU_2013
KP703957.1_BRSPGU_2013
KP703882.1_BRSPGU_2013
KP704043.1_BRSPGU_2013
KP704075.1_BRSPGU_2013
KP704116.1_BRSPGU_2013
KP703988.1_BRSPGU_2013
KP638367.1_BRSPSJ_2012
KP638365.1_BRSPSJ_2012
KP638368.1_BRSPSJ_2012
KJ596658.1_BRMTCU_2012
KJ579243.1_BRMTNL_2012
KJ596659.1_BRMTVG_2012
KP188565.1_BRSPSJ_2013
KP188566.1_BRSPSJ_2013
KU513441.1_BRPRCA_2013
KJ596672.1_BRMTVG_2012
KP188564.1_BRSPSJ_2013
KP638380.1_BRSPSJ_2013
KJ596661.1_BRMTCU_2012
JN848496.1_BRRSPA_2011
JQ513339.1_BRAMMA_2011
JQ513343.1_BRAMMA_2011
JN983813.1_BRRRBV_2010
JQ513333.1_BRRRBV_2010
JQ513337.1_BRPABE_2011
JQ513335.1_BRPABE_2011
JQ513334.1_BRPASA_2010
Clade II
Clade I
2007
2008
2009
2010
2011
2012
2013

Temporal dynamics of DENV-4 strains circulating in Brazil.

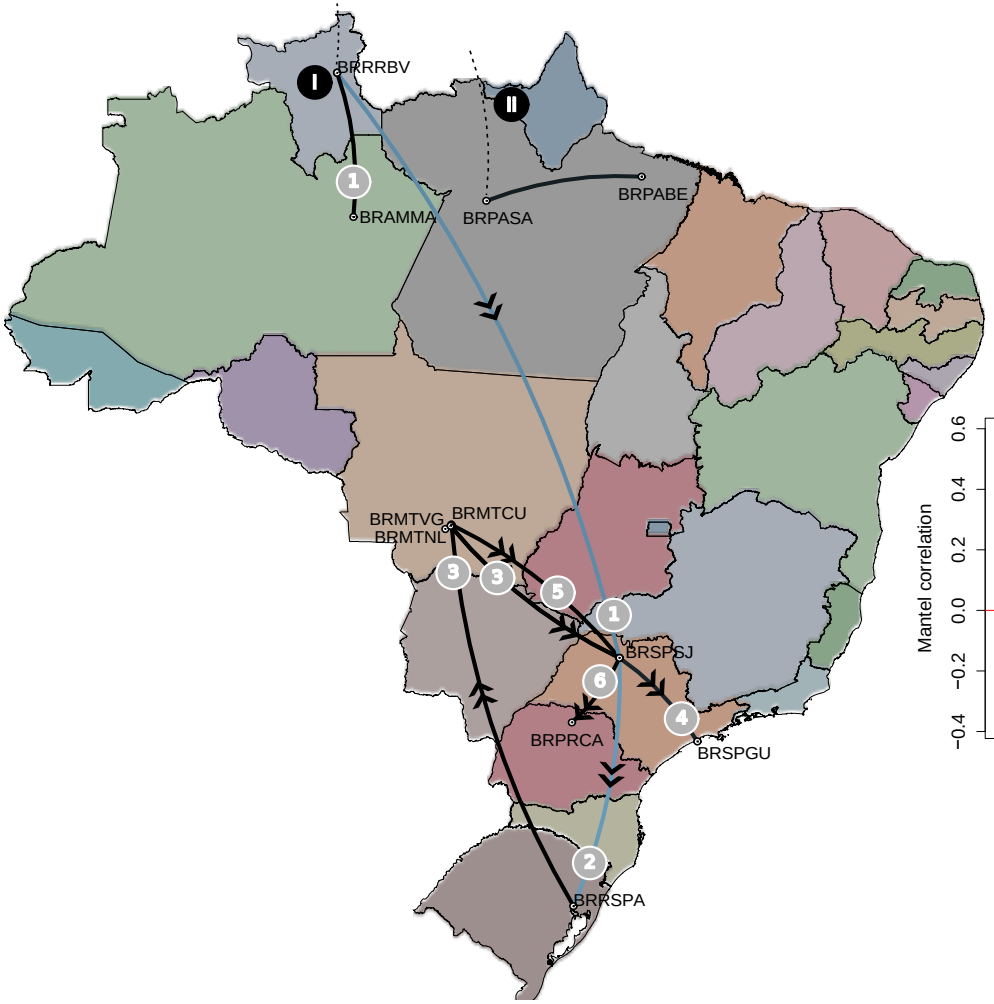

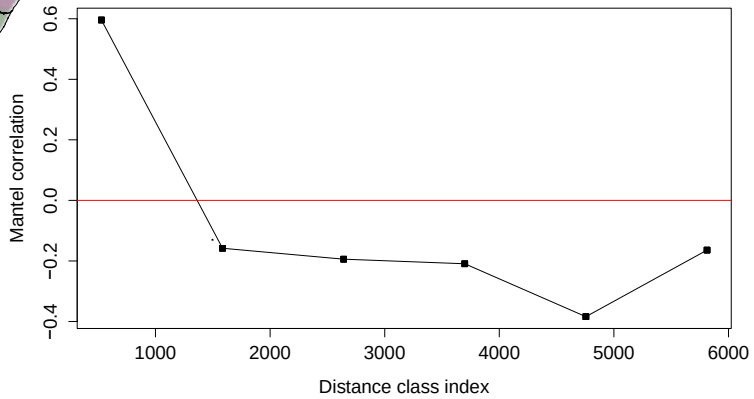

Mantel spatial correlogram:
patristic vs *geographic* distances

The numbers represent the chronological order of viral diffusion across the country. Posterior probability is indicated by line color. Blue: high supported migration (>0.70); cyan: low supported migration (>0.70).

ZIKV in Brazil: The issues…

- Causal relation of ZIKV & congenital ZIKV syndrome (CZS)
- ZIKV infection in 2-, 3-D systems, animal models, following "persistent" infections.
- Anti-ZIKV molecules & MAbs.
- Serological & molecular diagnostics tools (different platforms).
- Vaccine development (different platforms).
- Assemble & manage cohorts of pregnant women in consort with research groups.
- Entomology: control, vector genetics, physiology & ecology

>150 papers published since the second semester of 2015 in journals like Cell, Nature, The Lancet, Science, NEJM, &c.

"Brazilian storm" – Stevens Rehen

Funding research in Brazil

Main funding agencies:

- **CNPq** - Conselho Nacional de Desenvolvimento Científico e Tecnológico - "National Counsel of Technological and Scientific Development" (***cnpq****.br/*).

- **MS** – Ministério da Saúde – "Ministry of Health" (http://portalsaude.saude.gov.br/).

- **MCTIc** - Ministério da Ciência, Tecnologia, Inovações e Comunicações (http://www.mcti.gov.br/).

- **FAPESP** - Fundação de Amparo `a Pesquisa do Estado de São Paulo - "São Paulo Research Foundation" (*www.**fapesp**.br/en/*).

Viral Genetic Diversity Network (VGDN): the precursor of the FAPESP ZIKV network

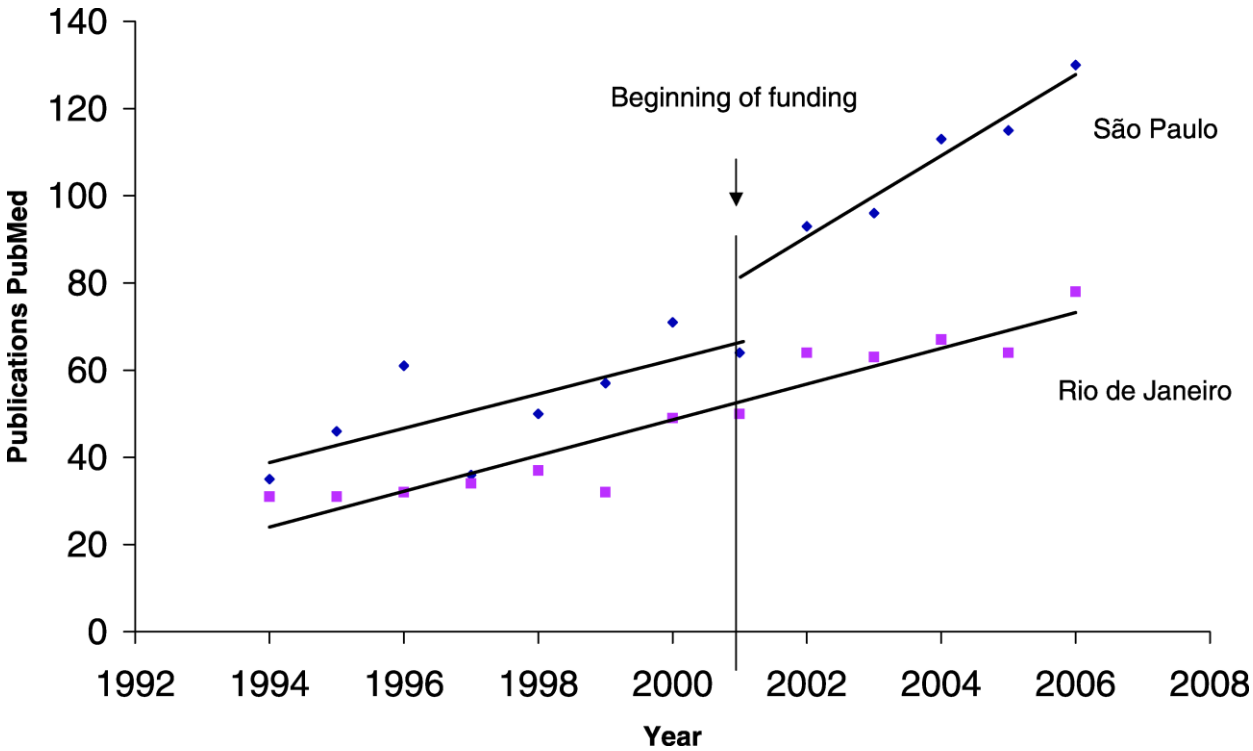

OPEN ACCESS Freely available online

PLoS BIOLOGY

Community Page

Boosting Virology in Brazil

Maria Inês de Moura Campos Pardini, Leda Fátima Jamal, Edison Luiz Durigon, Eduardo Massad, José Fernando Perez, João Renato Rebello Pinho, Edward C. Holmes, Paolo Marinho de Andrade Zanotto*

ZIKV network topology FAPESP

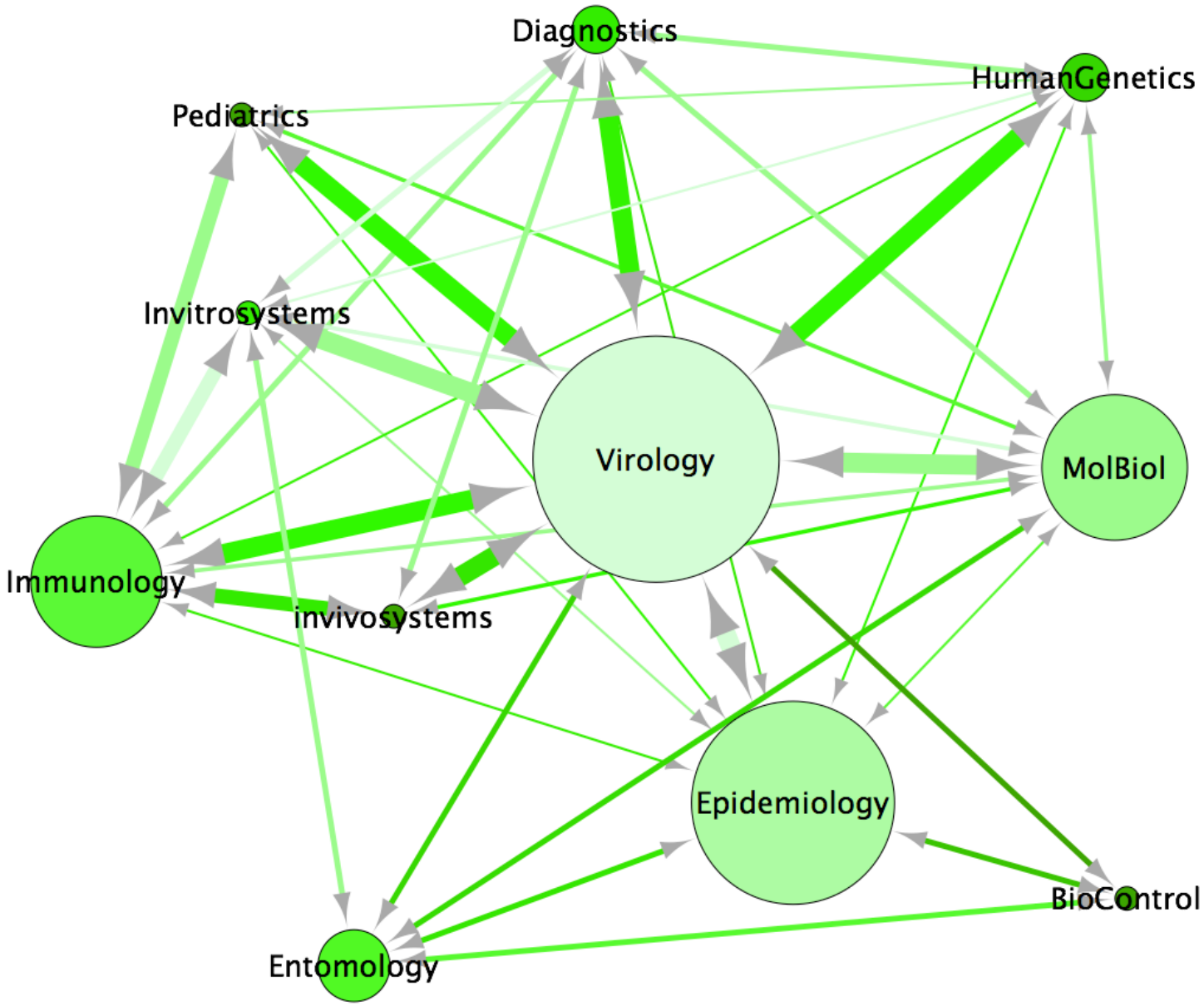

Freitas et al., JAMA Ophthalmol.
doi:10.1001/jamaophthalmol.2016.0267
Published online February 9, 2016.

Figure 3. Fundus Photographs of a 1-Month-Old Infant

A Right eye B Left eye

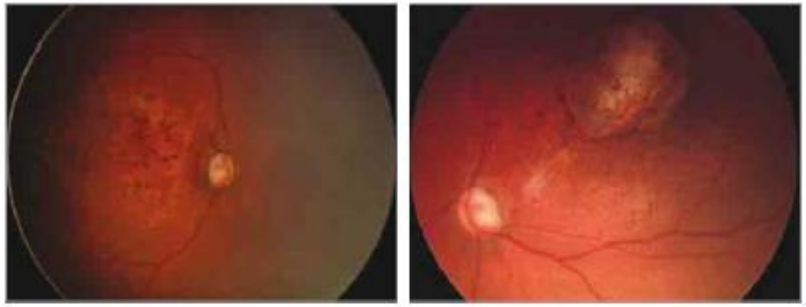

The right eye has an enlarged cup-disc ratio and macular pigmentary mottling (A), and the left eye has a roundish macular chorioretinal atrophic lesion with a hyperpigmented halo and pigmentary mottling, as well as an enlarged cup-disc ratio of the optic nerve.

Figure 4. Fundus Photographs of a 1-Month-Old Infant

A Right eye B Left eye

The right eye has a superotemporal perimacular chorioretinal scar with perilesional pigmentary mottling (A), and the left eye has similar findings (B).

Figure 5. Fundus Photographs of a 20-Day-Old Infant

A Right eye B Left eye

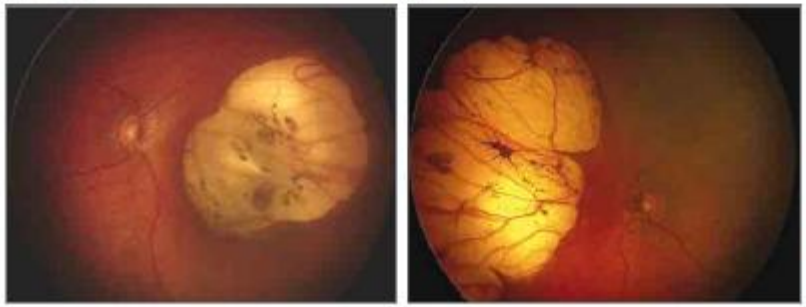

The right eye has optic disc hypoplasia, peripapillary nasal atrophy, and an excavated nasal round lesion with a hyperpigmented halo, with a coloboma-like aspect (A), and the left eye has optic disc hypoplasia, peripapillary nasal atrophy, and a retinal nasal lesion with a similar pattern (B).

Table. Ocular Findings in Infants With Microcephaly and Presumed Zika Virus Congenital Infection

Ocular Finding	Patient No. 1	2	3	4	5	6	7	8	9	10	Affected Eyes, No. (%) (n = 17)
Focal pigment mottling	OU	OD	OU	No	OU	OD	No	OU	OS	No	11 (64.7)
Chorioretinal atrophy	OU	OS	OU	OU	OS	No	OS	OU	No	No	11 (64.7)
Optic nerve abnormalities	OU	No	No	OU	OU	No	No	No	No	OU	8 (47.1)
Iris coloboma	No	No	No	No	No	OU	No	No	No	No	2 (11.8)
Lens subluxation	No	No	No	No	No	OS	No	No	No	No	1 (5.9)
Signs of active uveitis	No	No	No	No	No	No	No	No	No	No	0
Vasculitis	No	No	No	No	No	No	No	No	No	No	0

Abbreviations: OD, right eye; OS, left eye; OU, each eye.

Conclusions

In summary, 10 of 29 infants with microcephaly (34.5%) had severe ocular abnormalities; these infants were born after a ZIKV outbreak in the state of Bahia in Brazil. The posterior ocular findings were focal pigment mottling and chorioretinal atrophy with a predilection for the macular area, as well as optic disc abnormalities. These findings can contribute to the diagnosis of ZIKV congenital infection in children with congenital microcephaly, although the retinal lesions found in this sample may resemble West Nile virus or toxoplasmosis retinochoroiditis.[35] Advances in serologic ZIKV tests and additional studies are necessary to confirm such findings.

This study can help guide clinical management and practice, as we observed that a high proportion of the infants with microcephaly had ophthalmologic lesions. Infants with microcephaly should undergo routine ophthalmologic evaluations to identify such lesions. In high-transmission settings, such as South America, Central America, and the Caribbean, ophthalmologists should be aware of the risk of congenital ZIKV-associated ophthalmologic sequelae.

Instituto Evandro Chagas
MS- SECRETARIA DE VIGILÂNCIA EM SAÚDE
1936-2016

ULTRASOUND
in Obstetrics & Gynecology

Physician Alert

Zika virus intrauterine infection causes fetal brain abnormality and microcephaly: tip of the iceberg?

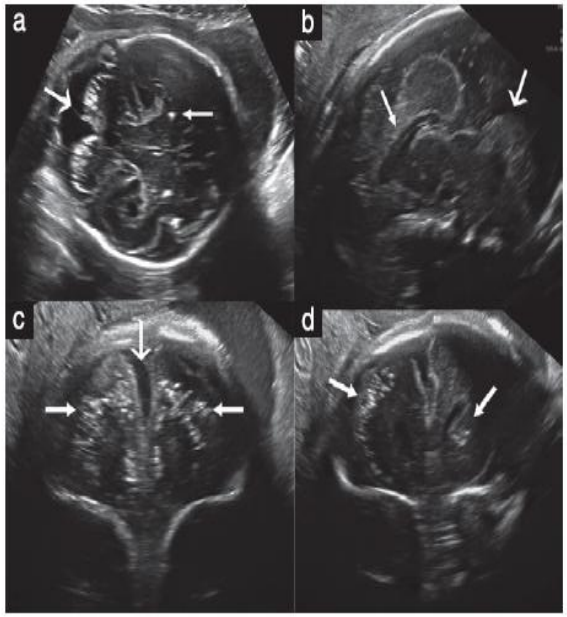

Figure 1 Case 1: (a) Transabdominal axial ultrasound image shows cerebral calcifications with failure of visualization of a normal vermis (large arrow). Calcifications are also present in the brain parenchyma (small arrow). (b) Transvaginal sagittal image shows dysgenesis of the corpus callosum (small arrow) and vermis (large arrow). (c) Coronal plane shows a wide interhemispheric fissure (large arrow) due to brain atrophy and bilateral parenchymatic coarse calcifications (small arrows). (d) Calcifications are visible in this more posterior coronal view and can be seen to involve the caudate (arrows).

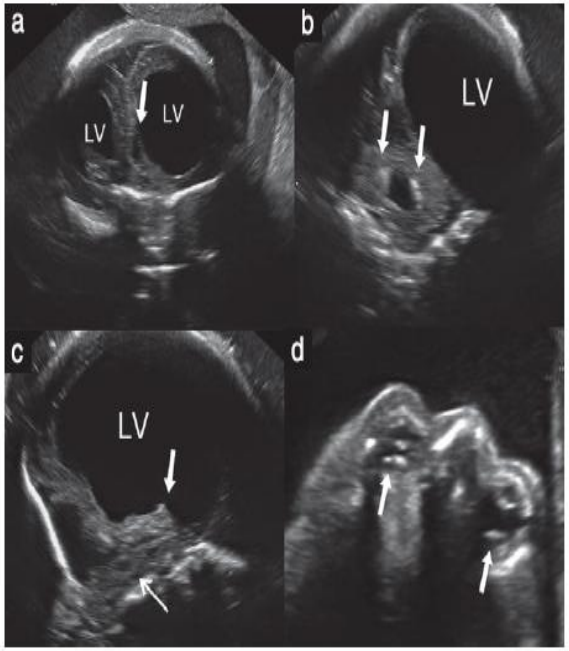

Figure 2 Case 2: (a) Anterior coronal view shows severe asymmetric ventriculomegaly with cystic formation (arrow). (b) Posterior horn of the lateral ventricle (LV) in coronal view is dilated. Note calcifications in the fourth ventricle (arrows). (c) The thalamus is absent (arrow) and the brainstem and pons are thin and difficult to visualize (sagittal view). (d) Axial view shows calcifications in both eyes (arrows). Note that the proximal eye is very small and lacks normal anatomic landmarks.

Oliveira Melo, A. S., Malinger, G., Ximenes, R., Szejnfeld, P. O., Alves Sampaio, S. and Bispo de Filippis, A. M

Ultrasound Obstet Gynecol 2016; **47**: 6–7

Instituto Evandro Chagas
MS- SECRETARIA DE VIGILÂNCIA EM SAÚDE
1936-2016

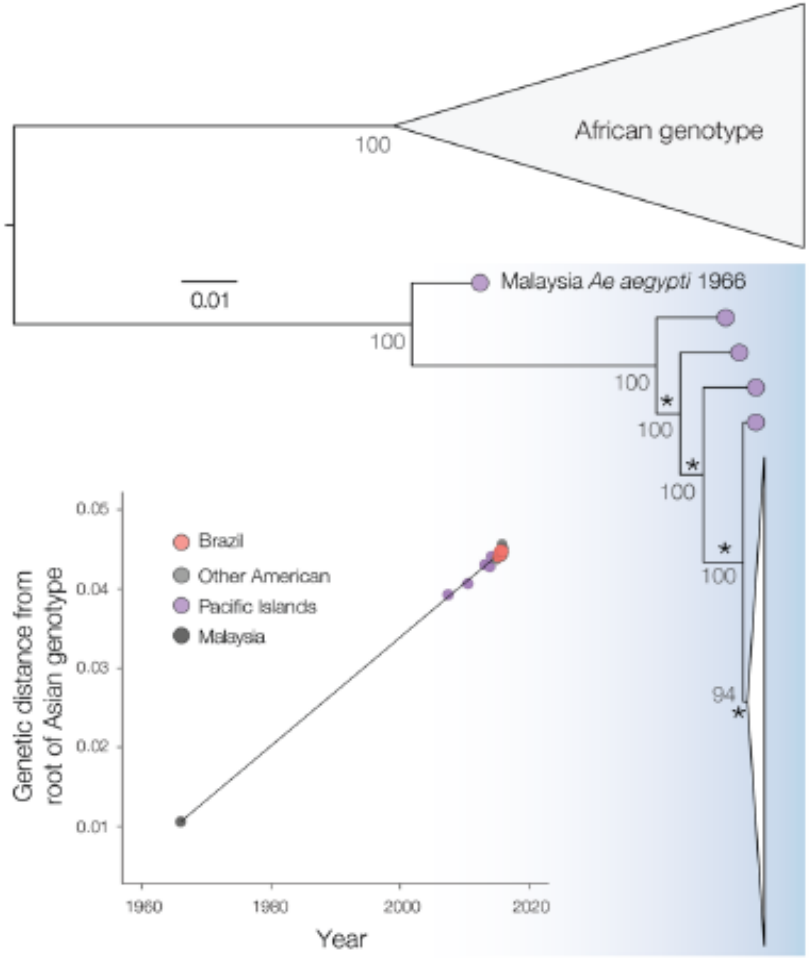

Fig. 2. Maximum likelihood phylogeny of ZIKV complete coding region sequences. Bootstrap scores are shown next to well-supported nodes and the phylogeny was mid-point rooted. A fully annotated tree is provided in fig. S2. The American ZIKV outbreak clade is drawn as a white triangle and is shown in detail in Fig. 3. Asterisks highlight the four internal branches that are ancestral to the American ZIKV lineage (see main text and fig. S3). Correlation between the sampling date of each sequence and the genetic distance of that sequence from the root of a maximum likelihood phylogeny of the Asian genotype (R^2 = 0.997). A molecular clock phylogeny of this data is shown in Fig. 3. The Malaysian strain (HQ234499) sampled in 1966 is the oldest representative of that genotype and falls on the regression line, indicating that it does not appear to be unusually divergent for its age. A similar analysis with the HQ234499 strain excluded is shown in fig. S5C.

Science REPORTS

Cite as: N. R. Faria *et al.*, *Science* 10.1126/science.aaf5036 (2016).

Zika virus in the Americas: Early epidemiological and genetic findings

Nuno Rodrigues Faria,[1,2*] Raimunda do Socorro da Silva Azevedo,[3*] Moritz U. G. Kraemer,[2] Renato Souza,[4] Mariana Sequetin Cunha,[4] Sarah C. Hill,[2] Julien Thézé,[2] Michael B. Bonsall,[2] Thomas A. Bowden,[5] Ilona Rissanen,[5] Iray Maria Rocco,[4] Juliana Silva Nogueira,[4] Adriana Yurika Maeda,[4] Fernanda Giselí da Silva Vasami,[4] Fernando Luiz de Lima Macedo,[4] Akemi Suzuki,[4] Sueli Guerreiro Rodrigues,[3] Ana Cecília Ribeiro Cruz,[3] Bruno Tardeli Nunes,[3] Daniele Barbosa de Almeida Medeiros,[3] Daniela Sueli Guerreiro Rodrigues,[3] Alice Louize Nunes Queiroz,[3] Eliana Vieira Pinto da Silva,[3] Daniele Freitas Henriques,[3] Elisabeth Salbe Travassos da Rosa,[3] Consuelo Silva de Oliveira,[3] Livia Caricio Martins,[3] Helena Baldez Vasconcelos,[3] Livia Medeiros Neves Casseb,[3] Darlene de Brito Simith,[3] Jane P. Messina,[2,6] Leandro Abade,[2] José Lourenço,[2] Luiz Carlos Junior Alcantara,[7] Maricélia Maia de Lima,[8] Marta Giovanetti,[7] Simon I. Hay,[9,3] Rodrigo Santos de Oliveira,[1] Poliana da Silva Lemos,[1] Layanna Freitas de Oliveira,[1] Clayton Pereira Silva de Lima,[1] Sandro Patroca da Silva,[1] Janaina Mota de Vasconcelos,[1] Luciano Franco,[1] Jedson Ferreira Cardoso,[1] João Lídio da Silva Gonçalves Vianez-Júnior,[1] Daiana Mir,[10] Gonzalo Bello,[10] Edson Delatorre,[10] Kamran Khan,[11,12] Marisa Creatore,[13] Giovanini Evelim Coelho,[14] Wanderson Kleber de Oliveira,[14] Robert Tesh,[15] Oliver G. Pybus,[2,6]†‡ Marcio R. T. Nunes,[1,15]†‡ Pedro F. C. Vasconcelos[1]†‡

[1]Center for Technological Innovation, Evandro Chagas Institute, Ministry of Health, Ananindeua, PA, 67030-000, Brazil. [2]Department of Zoology, University of Oxford, South Parks Road, Oxford, OX1 3PS UK. [3]Department of Arbovirology and Hemorrhagic Fevers, Evandro Chagas Institute, Ministry of Health, Ananindeua, Pará State, Brazil. [4]Instituto Adolfo Lutz, University of São Paulo, Brazil. [5]Wellcome Trust Centre for Human Genetics, University of Oxford, Oxford, UK. [6]Metabiota, San Francisco, CA 94104, USA. [7]Oswaldo Cruz Foundation (FIOCRUZ), Salvador, Bahia, Brazil. [8]Centre of Post Graduation in Collective Health, Department of Health, Universidade Estadual de Feira de Santana, Feira de Santana, Bahia, Brazil. [9]Institute for Health Metrics and Evaluation, University of Washington, Seattle, WA, USA. [10]Laboratório de AIDS and Imunologia Molecular, Instituto Oswaldo Cruz, FIOCRUZ, Rio de Janeiro, Brazil. [11]Li Ka Shing Knowledge Institute, St. Michael's Hospital, Toronto, Canada. [12]Department of Medicine, Division of Infectious Diseases, University of Toronto, Canada. [13]Dalla Lana School of Public Health, University of Toronto, Canada. [14]Brazilian Ministry of Health, Brasília, Brazil. [15]Department of Pathology, University of Texas Medical Branch, Galveston, TX, USA.

*These authors contributed equally to this work.

†These authors contributed equally to this work.

‡Correspondening author. E-mail: oliver.pybus@zoo.ox.ac.uk (O.G.P.); marcionunesbrasil@yahoo.com.br (M.R.T.N.); pedrovasconcelos@iec.pa.gov.br (P.F.C.V.)

Brazil has experienced an unprecedented epidemic of Zika virus (ZIKV), with ~30,000 cases reported to date. ZIKV was first detected in Brazil in May 2015 and cases of microcephaly potentially associated with ZIKV infection were identified in November 2015. Using next generation sequencing we generated seven Brazilian ZIKV genomes, sampled from four self-limited cases, one blood donor, one fatal adult case, and one newborn with microcephaly and congenital malformations. Phylogenetic and molecular clock analyses show a single introduction of ZIKV into the Americas, estimated to have occurred between May-Dec 2013, more than 12 months prior to the detection of ZIKV in Brazil. The estimated date of origin coincides with an increase in air passengers to Brazil from ZIKV endemic areas, and with reported outbreaks in Pacific Islands. ZIKV genomes from Brazil are phylogenetically interspersed with those from other South American and Caribbean countries. Mapping mutations onto existing structural models revealed the context of viral amino acid changes present in the outbreak lineage; however no shared amino acid changes were found among the three currently available virus genomes from microcephaly cases. Municipality-level incidence data indicate that reports of suspected microcephaly in Brazil best correlate with ZIKV incidence around week 17 of pregnancy, although this does not demonstrate causation. Our genetic description and analysis of ZIKV isolates in Brazil provide a baseline for future studies of the evolution and molecular epidemiology in the Americas of this emerging virus.

Instituto Evandro Chagas
MS- SECRETARIA DE VIGILÂNCIA EM SAÚDE
1936-2016

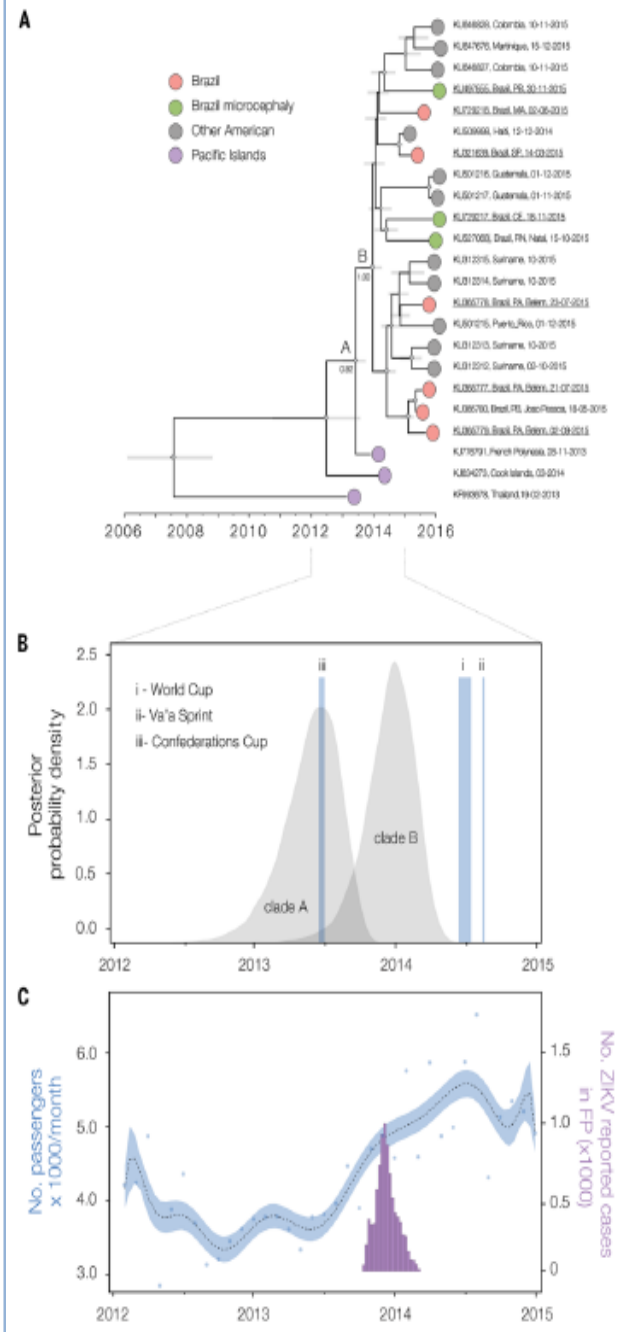

Fig. 3. Timescale of the introduction of ZIKV to the Americas. (A) Molecular clock phylogeny of the ZIKV outbreak lineage estimated from complete coding region sequences, plus 6 sequences (KJ634273, KU312315, KU312314, KU212313, KU646828, and KU646827) longer than 1500nt (available data as of 7th March 2016). For visual clarity, three basal sequences, HQ23499 (Malaysia, 1966), EU545988 (Micronesia, 2007) and JN860885 (Cambodia, 2010) are not displayed here (see fig. S3). Gray horizontal bars represent 95% Bayesian credible intervals for divergence dates. A and B denote clades discussed in main text and numbers next to them denote posterior probabilities. Diamond sizes represent, at each node, the posterior probability support of that node. Taxa are labeled with accession number, sampling location, and sampling date. Names of sequences generated in this study are underlined. (B) Posterior distributions of the estimated ages (TMRCAs) of clades A and B, estimated in BEAST using under the best fitting evolutionary model (table S2). The time and duration of the three events (i-iii) discussed in the main text are shown. (C) The blue curve (left hand axis) shows a polynomial fitting of the number of travelers (blue points) from countries with recorded ZIKV outbreaks between 2012 and 2015 (French Polynesia, Thailand, Indonesia, Malaysia, Cambodia, New Caledonia, supplementary materials section 6), aggregated across 20 Brazilian national airports. The purple bars represent weekly numbers of suspected ZIKV cases (right hand side) in French Polynesia from the 30 Oct 2013 to 14 Feb 2014 (4).

Faria et al., Science, 2016.

Instituto Evandro Chagas
MS- SECRETARIA DE VIGILÂNCIA EM SAÚDE
1936-2016

JIDC | THE JOURNAL OF INFECTION IN DEVELOPING COUNTRIES

Emerging Problems in Infectious Diseases

Zika virus infection, associated microcephaly, and low yellow fever vaccination coverage in Brazil: is there any causal link?

Luciano Pamplona de Góes Cavalcanti[1], Pedro Luiz Tauil[5], Carlos Henrique Alencar[1], Wanderson Oliveira[2], Mauro Martins Teixeira[3], Jorg Heukelbach[1,4]

[1] *Department of Community Health, School of Medicine, Federal University of Ceará, Fortaleza, CE, Brazil*
[2] *Coordenação Geral de Vigilância e Resposta às Emergências em Saúde Pública do Ministério da Saúde do Brasil, Brasília, Brazil*
[3] *Department of Biochemistry and Immunology, Biological Science Institute, Federal University of Minas Gerais, Belo Horizonte, Minas Gerais, Brazil*
[4] *Anton Breinl Centre for Public Health and College of Public Health, Medical and Veterinary Sciences, Division of Tropical Health and Medicine, James Cook University, Townsville, Queensland, Australia*
[5] *Faculty of Medicine, University of Brasília (UnB), Distrito Federal, DF, Brazil*

Abstract

Introduction: Since the end of 2014, Zika virus (ZIKV) infection has been rapidly spreading in Brazil.

Methodology: To analyze the possible association of yellow fever vaccine with a protective effect against ZIKV-related microcephaly, the following spatial analyses were performed, using Brazilian municipalities as units: i) yellow fever vaccination coverage in Brazilian municipalities in individuals aged 15-49; ii) reported cases of microcephaly by municipality; and iii) confirmed cases of microcephaly related to ZIKV, by municipality. SaTScan software was used to identify clusters of municipalities for high risk of microcephaly.

Results: There were seven significant high risk clusters of confirmed microcephaly cases, with four of them located in the Northeast where yellow fever vaccination rates were the lowest. The clusters harbored only 2.9% of the total population of Brazil, but 15.2% of confirmed cases of microcephaly.

Conclusion: We hypothesize that pregnant women in regions with high yellow fever vaccination coverage may pose their offspring to lower risk for development of microcephaly. There is an urgent need for systematic studies to confirm the possible link between low yellow fever vaccination coverage, Zika virus infection and microcephaly.

Figure 1. (**A**) Yellow fever vaccination coverage in individuals aged 15-49 in Brazil; (**B**) reported cases of microcephaly between October 2015 and March 2016; (**C**) confirmed cases of microcephaly between October 2015 and March 2016; (**D**) clusters of confirmed cases of microcephaly associated with ZIKV; arrows indicate location of clusters. Observation units are the 5,570 municipalities of Brazil.

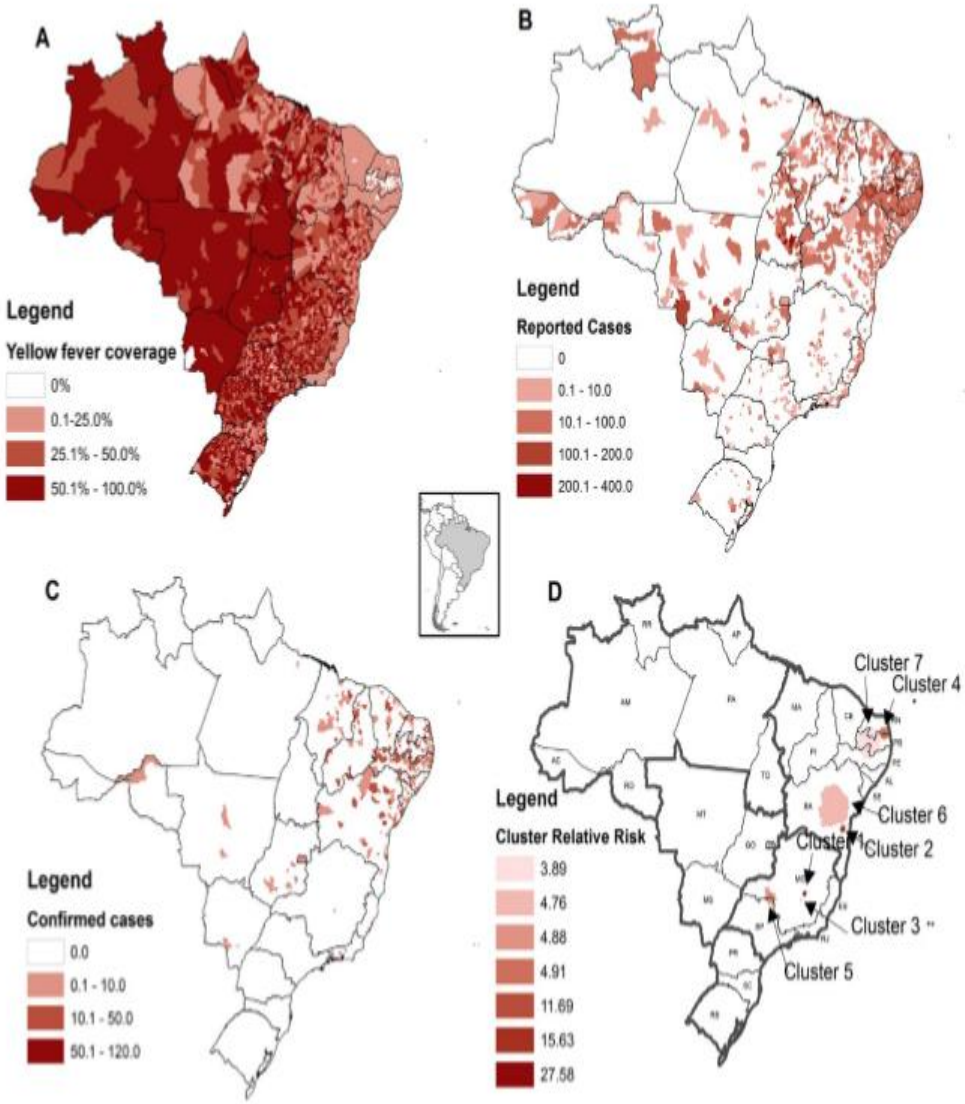

Zika virus damages the human placental barrier and presents marked fetal neurotropism

Lucia de Noronha[1], Camila Zanluca[2], Marina Luize Viola Azevedo[1], Kleber Giovanni Luz[3], Claudia Nunes Duarte dos Santos[2]/+

[1]Pontifícia Universidade Católica do Paraná, Curitiba, PR, Brasil [2]Fundação Oswaldo Cruz, Instituto Carlos Chagas, Laboratório de Virologia Molecular, Curitiba, PR, Brasil [3]Universidade Federal do Rio Grande do Norte, Instituto de Medicina Tropical, Natal, RN, Brasil

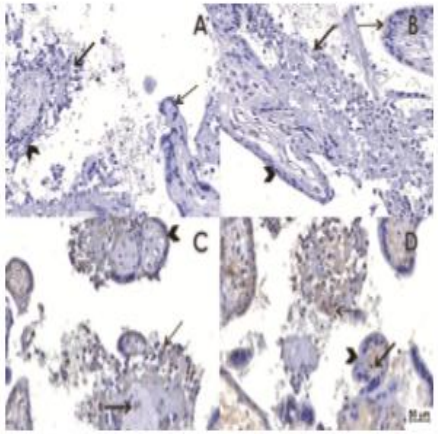

Fig. 1: pathological findings and immunohistochemistry reactions in placental tissues. (A) Histological section of case 1 immunostained by the conventional immunohistochemistry technique, omitting the primary antibody, which was used as a negative control. We observed chronic placentitis (TORCH type) with chronic villous inflammation (histiocytic-predominant villitis - arrow), edema and trophoblastic epithelial lesions (arrow head) as compared to normal villous tissue (dashed arrow). There was an increase in villous Hofbauer cells and villous stromal lymphohistiocytic cells. (B) Histological section of case 1 immunostained with a non-related anti-Chikungunya virus monoclonal antibody as the primary antibody, which was used as a negative control. We observed the same features observed in A (arrow shows histiocytic-predominant villitis, arrow head shows non lesional trophoblastic epithelial cells and dashed arrow shows normal villi). (C-D) Histological section of case 1 immunostained with the anti-flavivirus monoclonal antibody 4G2. Chronic placentitis (TORCH-type) was observed with immunopositivity in Hofbauer cells (arrow) and some histiocytes in the intervillous spaces (dashed arrow). There was no immunopositivity in the trophoblastic epithelium (arrow head).

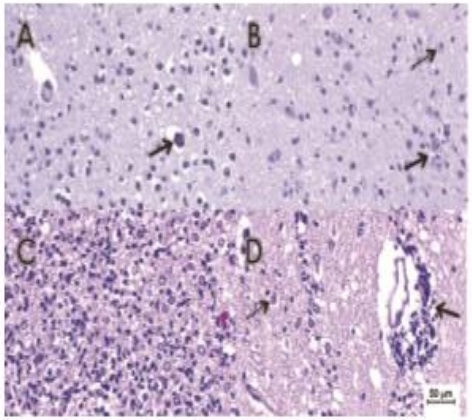

Fig. 2: anatomopathological findings on brain tissues samples stained with H&E. (A) Histological section of brain tissue samples of case 2 with a mildly affected white matter region revealing diffuse microglial hyperplasia, gliosis with reactive astrocytes and microdeposits of calcium (arrow). (B) Histological section of a brain tissue sample from case 3 with a mildly affected white matter region containing microglial nodules (arrow) and neuronophagia (dashed arrow). (C) Histological section of a brain tissue sample from case 4 with a more severely affected white matter region, revealing extensive destruction and infiltration by mononuclear inflammatory cells. Diffuse microglial hyperplasia was also present. In addition, severe gliosis with reactive gemistocytic astrocytes were diffusely distributed. (D) Histological section of a brain tissue sample from case 4 with a more severely affected white matter region showing extensive perivascular cuffing by lymphocytes (arrow). In addition, moderate gliosis with reactive gemistocytic astrocytes (dashed arrow) were diffusely distributed.

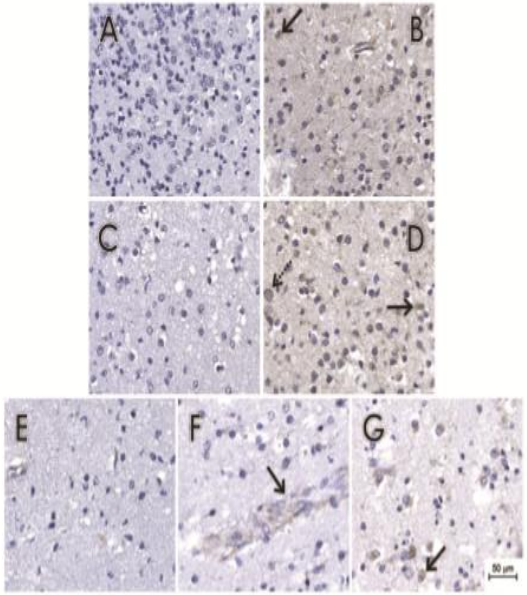

Fig. 3: pathological findings and immunohistochemical reactions in brain tissues. (A-D) Histological sections of brain tissue samples of cases 2 (A-B) and 3 (C-D) immunostained with 4G2 (B and D) or with a non-related anti-Chikungunya virus monoclonal antibody (A and C). We observed some positive glial cells (arrow) and scattered foci of microcalcifications (dashed arrows). (E-G) Histological sections of brain tissue samples of case 4 immunostained with 4G2 (F-G) or with a non-related anti-Chikungunya virus monoclonal antibody (E) as the primary antibody. We observed some positive gemistocytic glial cells (G - arrow). We also observed scattered positive endothelial cells (F - arrow).

Is CZS caused by ZIKV?

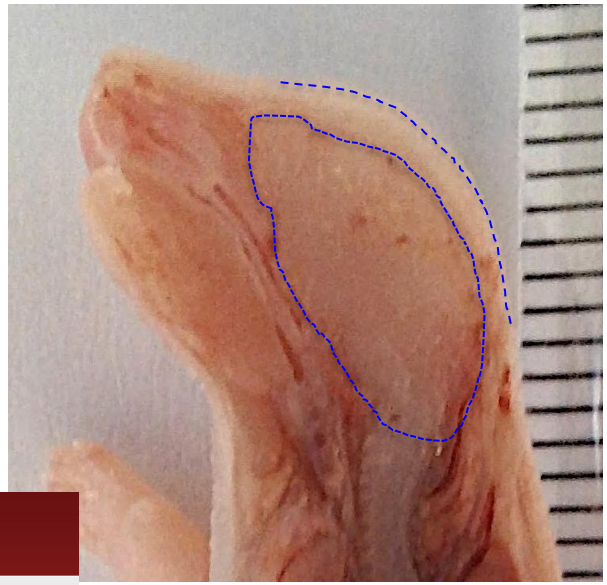

nature International weekly journal of science

Menu

archive ▸ volume 534 ▸ issue 7606 ▸ letters ▸ article

ARTICLE PREVIEW

view full access options ▸

NATURE | LETTER

日本語要約

The Brazilian Zika virus strain causes birth defects in experimental models

Fernanda R. Cugola, Isabella R. Fernandes, Fabiele B. Russo, Beatriz C. Freitas, João L. M. Dias, Katia P. Guimarães, Cecília Benazzato, Nathalia Almeida, Graciela C. Pignatari, Sarah Romero, Carolina M. Polonio, Isabela Cunha, Carla L. Freitas, Wesley N. Brandão, Cristiano Rossato, David G. Andrade, Daniele de P. Faria, Alexandre T. Garcez, Carlos A. Buchpigel, Carla T. Braconi, Erica Mendes, Amadou A. Sall, Paolo M. de A. Zanotto, Jean Pierre S. Peron, Alysson R. Muotri *et al.*

Affiliations | Contributions | Corresponding authors

Nature **534**, 267–271 (09 June 2016) | doi:10.1038/nature18296

Received 08 March 2015 | Accepted 04 May 2016 | Published online 11 May 2016

size reduction of brains

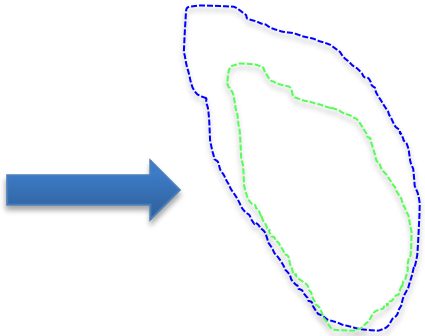

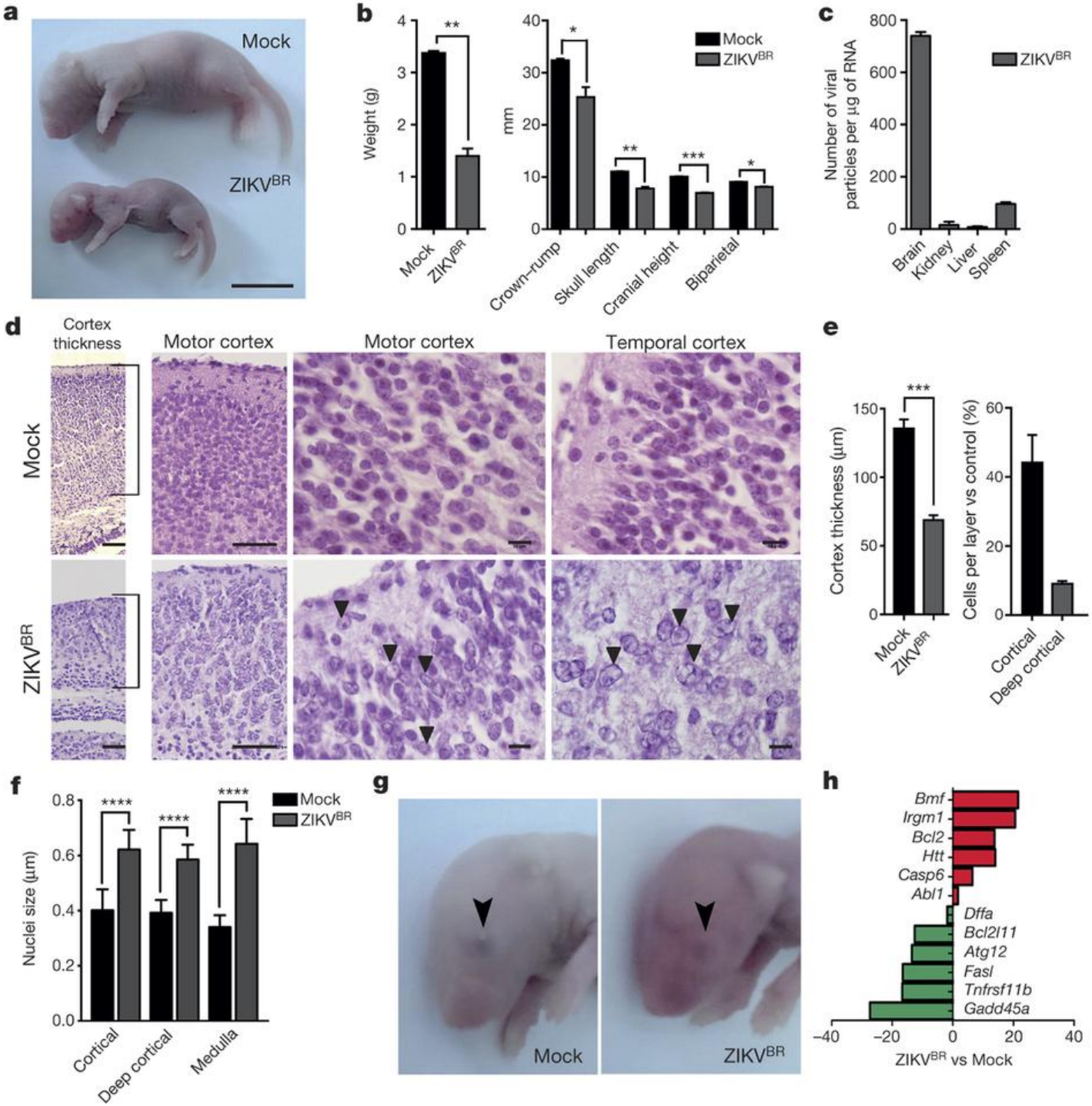
a
Mock
ZIKV^BR
b
Weight (g)
Mock
ZIKV^BR
mm
Crown–rump
Skull length
Cranial height
Biparietal
c
Number of viral particles per µg of RNA
ZIKV^BR
Brain
Kidney
Liver
Spleen
d
Cortex thickness
Motor cortex
Motor cortex
Temporal cortex
Mock
ZIKV^BR
e
Cortex thickness (µm)
Cells per layer vs control (%)
Mock
ZIKV^BR
Cortical
Deep cortical
f
Nuclei size (µm)
Mock
ZIKV^BR
Cortical
Deep cortical
Medulla
g
Mock
ZIKV^BR
h
Bmf
Irgm1
Bcl2
Htt
Casp6
Abl1
Dffa
Bcl2l11
Atg12
Fasl
Tnfrsf11b
Gadd45a
ZIKV^BR vs Mock

MOI calculation for ZIKV infection in 3D-systems

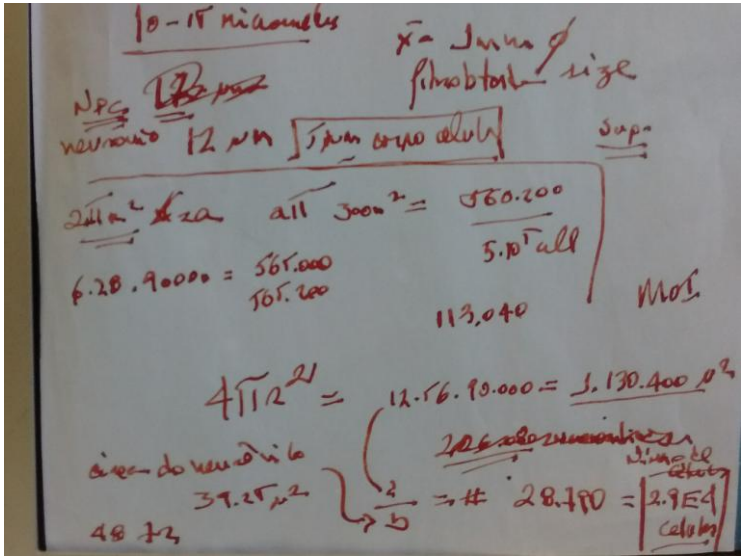

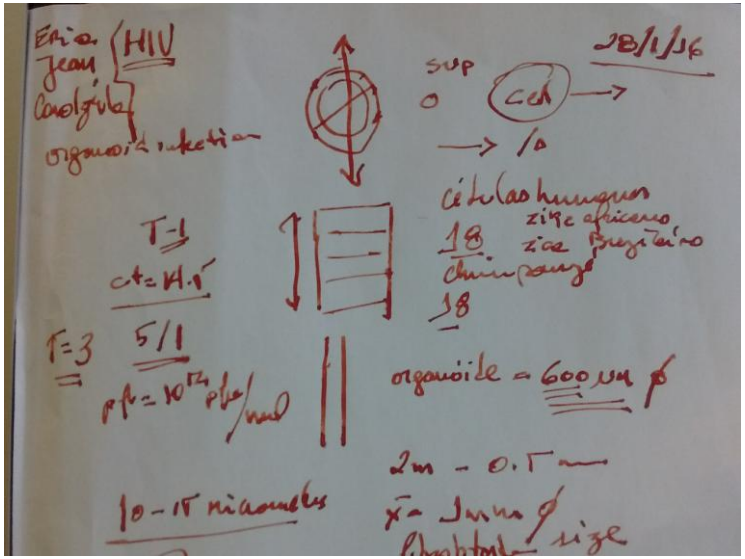

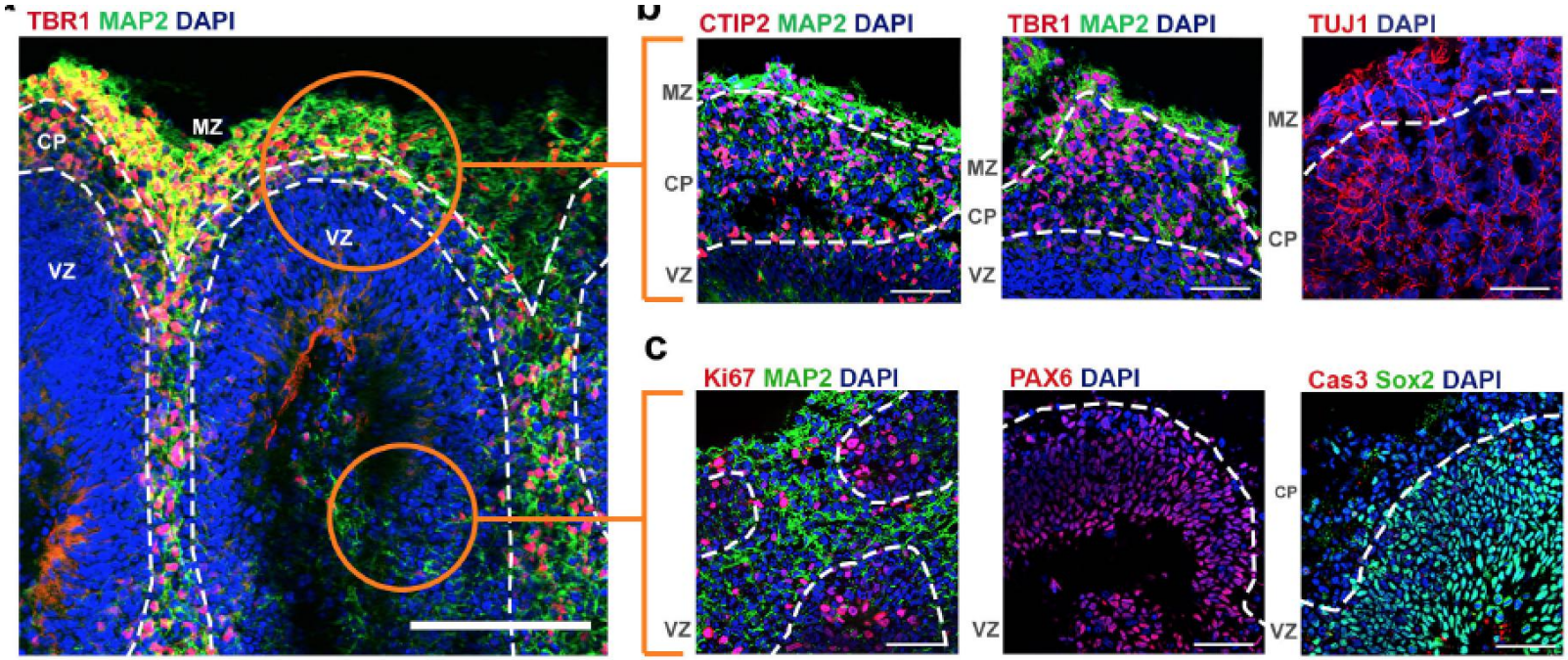

CORRESPONDENCE

Prolonged Shedding of Zika Virus Associated with Congenital Infection

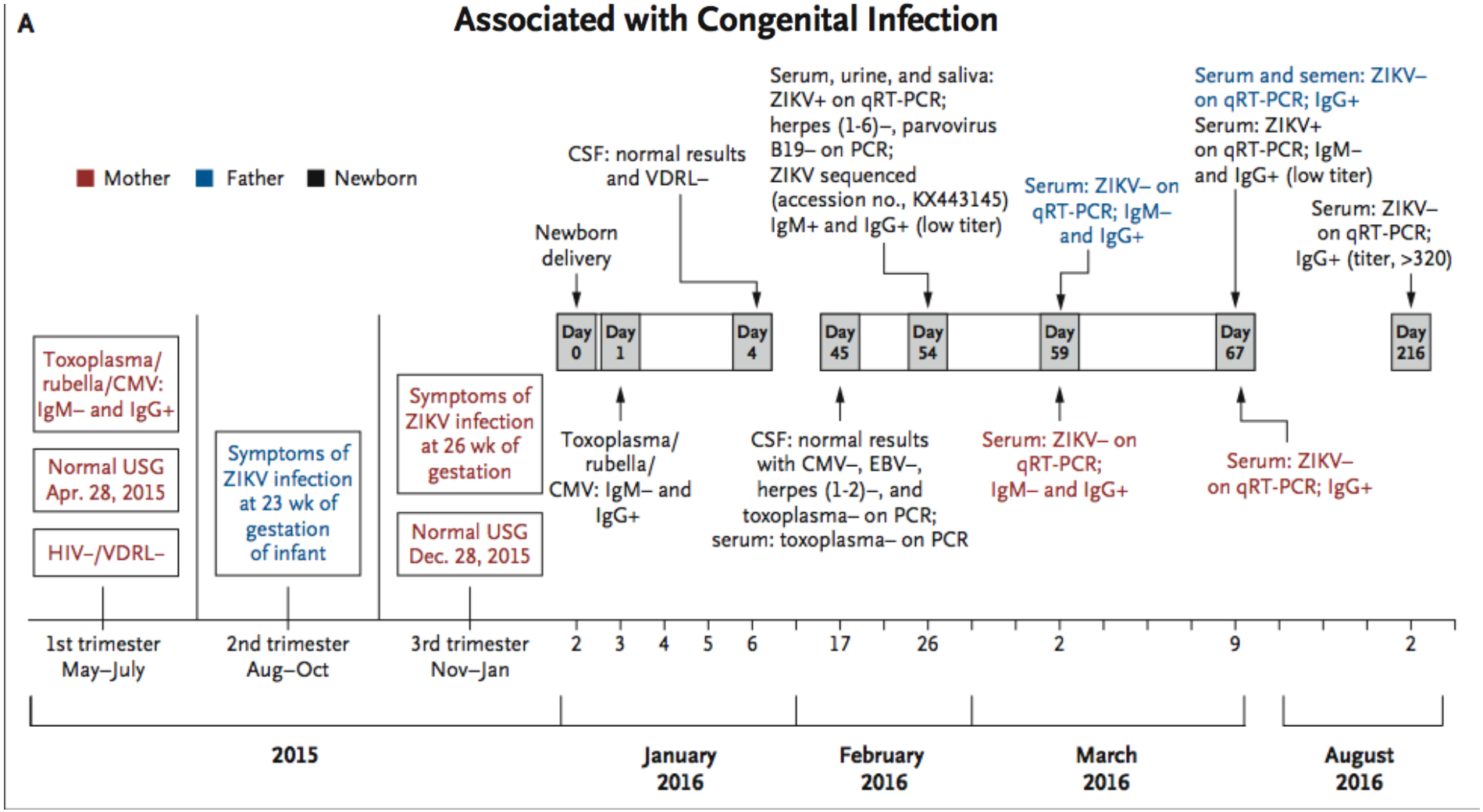

nature International weekly journal of science

Menu ▸ Advanced search Search

archive ▸ volume 536 ▸ issue 7617 ▸ letters ▸ article

ARTICLE PREVIEW

view full access options ▸

NATURE | LETTER

日本語要約

Vaccine protection against Zika virus from Brazil

Rafael A. Larocca Peter Abbink Jean Pierre S. Peron Paolo M. de A. Zanotto M. Justin Iampietro Alexander Badamchi-Zadeh Michael Boyd David Ng'ang'a Marinela Kirilova Ramya Nityanandam Noe B. Mercado Zhenfeng Li Edward T. Moseley Christine A. Bricault Erica N. Borducchi Patricia B. Giglio David Jetton George Neubauer Joseph P. Nkolola Lori F. Maxfield Rafael A. De La Barrera Richard G. Jarman Kenneth H. Eckels Nelson L. Michael Stephen J. Thomas Dan H. Barouch

Affiliations | Contributions | Corresponding author

Nature **536**, 474–478 (25 August 2016) | doi:10.1038/nature18952

Science

RESEARCH ARTICLES

Cite as: Abbink *et al.*, *Science* 10.1126/science.aah6157 (2016).

Protective efficacy of multiple vaccine platforms against Zika virus challenge in rhesus monkeys

Peter Abbink,[1*] Rafael A. Larocca,[1*] Rafael A. De La Barrera,[2] Christine A. Bricault,[1] Edward T. Moseley,[1] Michael Boyd,[1] Marinela Kirilova,[1] Zhenfeng Li,[1] David Ng'ang'a,[1] Ovini Nanayakkara,[1] Ramya Nityanandam,[1] Noe B. Mercado,[1] Erica N. Borducchi,[1] Arshi Agarwal,[1] Amanda L. Brinkman,[1] Crystal Cabral,[1] Abishek Chandrashekar,[1] Patricia B. Giglio,[1] David Jetton,[1] Jessica Jimenez,[1] Benjamin C. Lee,[1] Shanell Mojta,[1] Katherine Molloy,[1] Mayuri Shetty,[1] George H. Neubauer,[1] Kathryn E. Stephenson,[1] Jean Pierre S. Peron,[3] Paolo M. de A. Zanotto,[3] Johnathan Misamore,[4] Brad Finneyfrock,[4] Mark G. Lewis,[4] Galit Alter,[5] Kayvon Modjarrad,[2,6] Richard G. Jarman,[2] Kenneth H. Eckels,[2] Nelson L. Michael,[2] Stephen J. Thomas,[2†] Dan H. Barouch[1,5†‡]

Zika Virus (ZIKV) codon adaptation and fitness

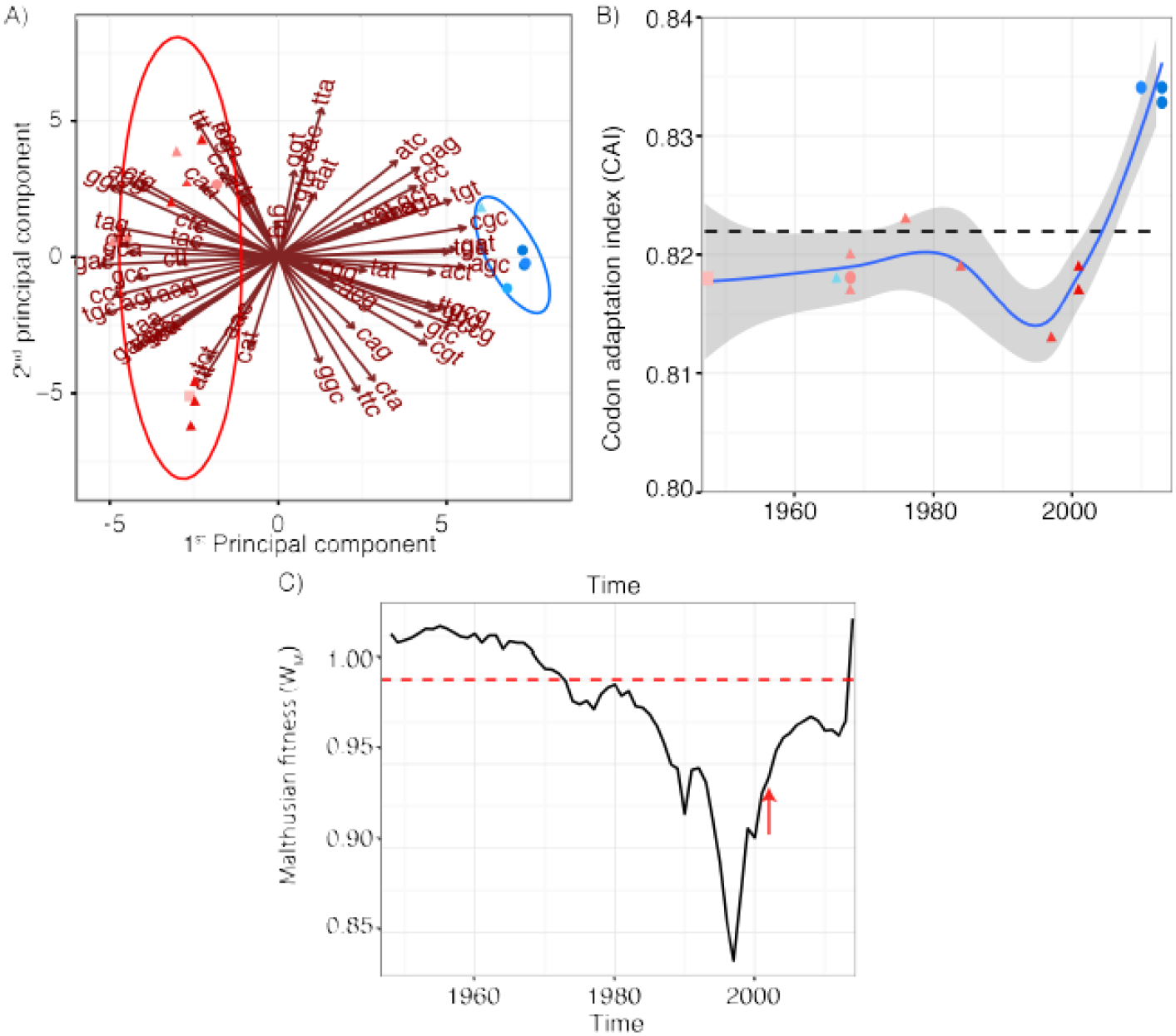

Intra-host ZIKV polymorphisms

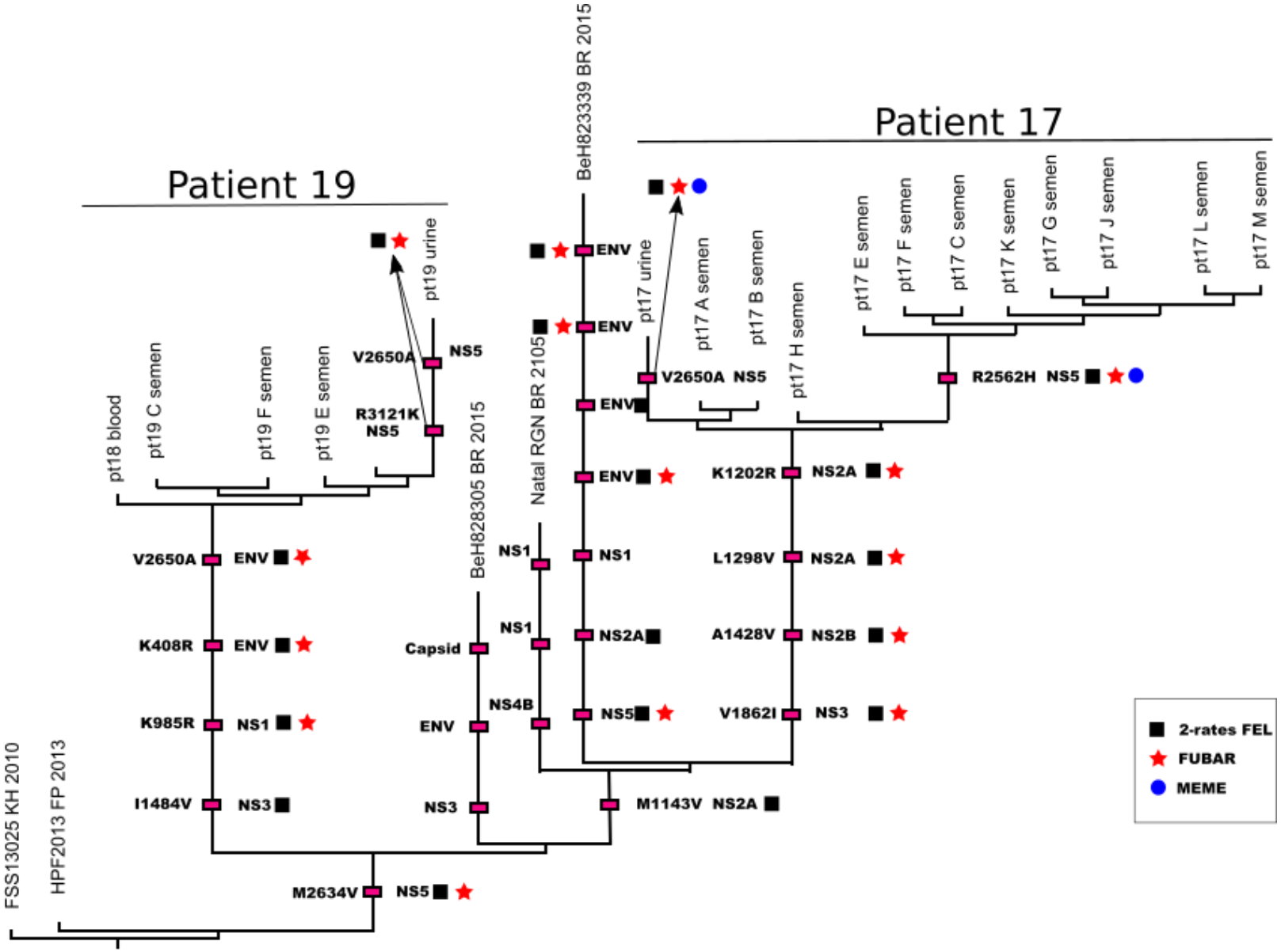

Inter- & Intra-host ZIKV diversity

Patient 17 - 237 days

Patients 19 & 18 - 155 days

Mean distance within groups:

Intra host
d : 0.00237 s/s
IS.E : 0.00033

Inter host
d : 0.00318 s/s
S.E : 0.00037

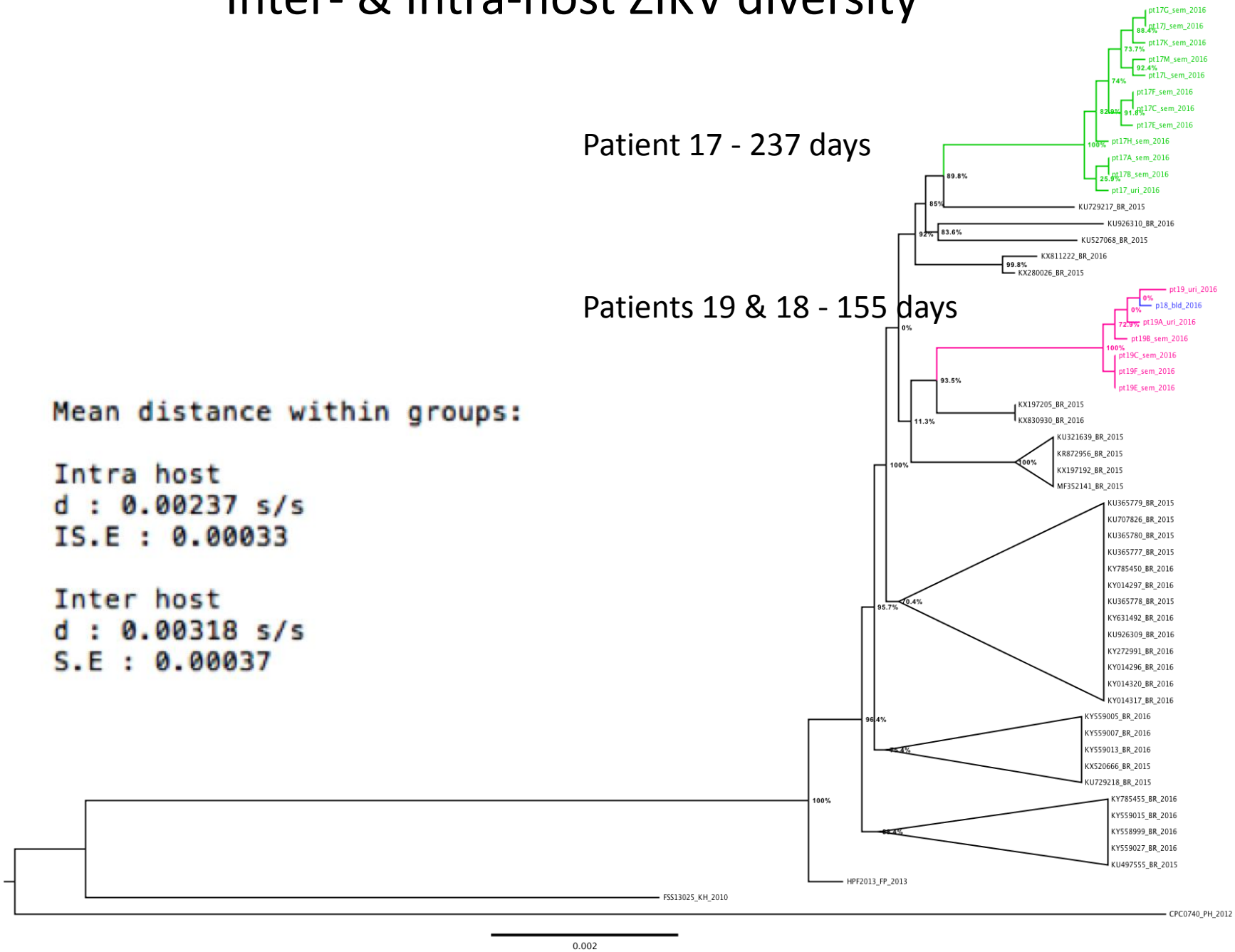

Conclusions

- Phylodynamics of flaviviruses works! Due to stable rates of change, stable nucleotide composition, insignificant recombination systematic error.
- Real time follow-up of dengue outbreaks can be useful for control: Guarujá stands as a proof of concept.
- ZIKV intra host evolution is similar to other RNA viruses.
- We need to incorporate viral genealogy & patient data to better understand the evolution of an outbreak.
- “Where there is no overlap there is gap” – Mark Miller, MD.

Acknowledgments

ACADEMIA BRASILEIRA DE CIÊNCIAS!

Christian Julián Villabona-Arenas
Suzanne Ortiz
Edison Durigon
Erica Mendes
Caio César de Melo Freire
Carla T. Braconi
Virologia, Departamento de Microbiologia, Instituto de Ciências Biomédicas, Universidade de São Paulo

Carla de Sousa Capra
Laboratório de Saúde Pública, Secretaria da Saúde, Prefeitura Municipal de Guarujá

Karime Balarini
Celso Ricardo Theoto P. Fonseca
Itapema Laboratório de Análises Clínicas, Guarujá

Mauricio Loureiro
Saulo Duarte Passos
Laboratório de Infectologia Pediátrica, Faculdade de Medicina de Jundiaí

Projeto FAPESP Nº 2014/17766-9
Projeto CNPq 441105/2016-5